

URSA: Understanding and Verifying Chain-of-thought Reasoning in Multimodal Mathematics

Ruilin Luo^{1,2*} Zhuofan Zheng^{2*} Yifan Wang¹ Yiyao Yu¹ Xinzhe Ni¹ Zicheng Lin¹ Jin Zeng² Yujiu Yang¹

Abstract

Chain-of-Thought (CoT) reasoning has emerged as a powerful technique for enhancing the mathematical reasoning capabilities of Large Language Models (LLMs). Recent advancements in process supervision for CoT trajectories have sparked significant interest in improving test-time scaling, thereby enabling System 2-style thinking in these models. However, in the context of multimodal mathematical reasoning, the lack of high-quality CoT training data has limited the ability of existing models to achieve both deliberate reasoning and fine-grained verification. In this paper, we introduce a three-module CoT data synthesis process, which combines CoT distillation, CoT-trajectory rewriting, and format unification to generate MMathCoT-1M, a high-quality CoT reasoning instruction fine-tuning dataset. Additionally, we develop a dual-view trajectory labeling automation mechanism that ensures both visual grounding fidelity and deductive chain validity, resulting in the DualMath-1.1M dataset. The URSA-8B model, trained on MMathCoT-1M, achieves state-of-the-art performance among similarly sized Multimodal Large Language Models (MLLMs) across six popular reasoning benchmarks. Further training URSA-8B on the DualMath-1.1M dataset yields URSA-RM-8B, a verifier model that enhances URSA-8B’s test-time performance and outperforms strong closed-source MLLMs, such as GPT-4o. Code, models and data can be found at <https://github.com/URSA-MATH/URSA-MATH>.

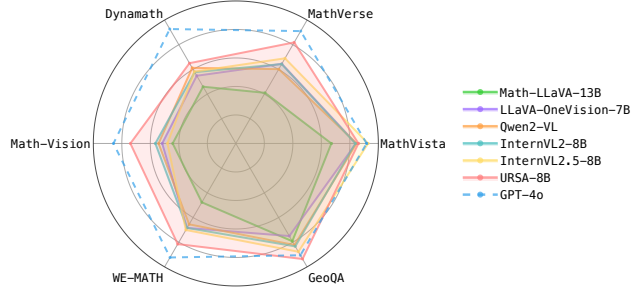


Figure 1: Performance comparison on six commonly used multimodal mathematical benchmarks.

1. Introduction

Chain-of-thought (CoT) reasoning has demonstrated significant effectiveness in enhancing mathematical reasoning capabilities within Large Language Models (LLMs) (Zhang et al., 2024e; Wei et al., 2022; Chu et al., 2023; Sprague et al., 2024; Zhang et al., 2022; An et al., 2023; Luo et al., 2024b; Mu et al., 2024). Recent studies have increasingly focused on supervising the quality of CoT trajectories during inference to facilitate system 2-style deliberate reasoning (Zhang et al., 2024b; Lightman et al., 2023; Setlur et al., 2024; Fu et al., 2024b). However, the application of this approach to mathematical reasoning in Multimodal Large Language Models (MLLMs) remains underexplored.

We identify two critical limitations in existing research: (i) Current multimodal math MLLMs have not shown a substantial improvement in reasoning performance compared to general-purpose MLLMs. This limitation may stem from the scarcity of high-quality CoT data, resulting in mixed training styles that inconsistently combine CoT-format reasoning and direct answer generation (Zhang et al., 2024e; Yang et al., 2024a; Zhang et al., 2023); (ii) In multimodal contexts, it remains unclear whether additional supervisory mechanisms are necessary beyond ensuring logical correctness, particularly for capturing new information inherent in multimodal inputs (Yan et al., 2024).

To address the first limitation, we propose a three-module CoT data synthesis framework designed to process diverse types of open-source data, culminating in the creation of

*Equal contribution. Work done during Ruilin’s internship at ByteDance. ¹Tsinghua University ²ByteDance. Correspondence to: Yujiu Yang <yang.yujiu@sz.tsinghua.edu.cn>, Co-First Author: <lrl23@mails.tsinghua.edu.cn>.

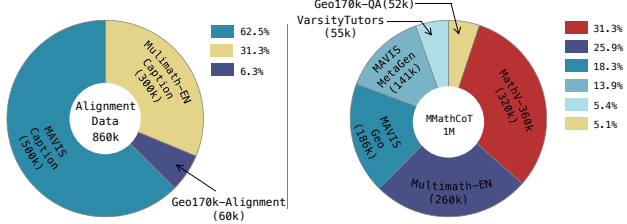


Figure 2: Data sources used by the URSA-8B model during the VL-alignment and SFT phases.

the MMathCoT-1M dataset (Peng et al., 2024; Zhang et al., 2024d; Zhuang et al., 2024; Shi et al., 2024). This framework integrates CoT distillation, trajectory rewriting, and format unification, aiming to enhance the foundational capabilities of math MLLMs and implicitly elevate their performance ceiling prior to the introduction of system 2-style slow reasoning.

For the second limitation, we introduce a dual-supervision mechanism that ensures both visual grounding fidelity and deductive chain validity. This is achieved by combining Monte Carlo Tree Search (MCTS)-based error localization with step-level targeted hallucination injection (Wang et al., 2024c; Gao et al., 2024; Liang et al., 2024; Browne et al., 2012). This approach enables the verifier to identify both perceptual and logical inconsistencies in reasoning processes. Metaphorically, our Process Reward Model (PRM) is designed to reward not only “doing things right” but also “seeing things accurately”. As a result, we develop the DualMath-1.1M dataset.

We propose a three-stage training pipeline comprising vision-language alignment, math-domain supervised fine-tuning, and PRM training. The latter two stages yield the URSA-8B and URSA-RM-8B models, respectively. As illustrated in Figure 1, we evaluate URSA-8B on six widely-used datasets, including MathVista (Lu et al., 2023a), MathVerse (Zhang et al., 2025), WE-MATH (Qiao et al., 2024), DYNAMATH (Zou et al., 2024), GeoQA (Chen et al., 2021), and Math-Vision (Wang et al., 2024a). URSA-8B achieves state-of-the-art (SOTA) performance among models of comparable size. Furthermore, URSA-RM-8B facilitates URSA-8B in performing robust system 2-style reasoning, enabling it to surpass the performance of GPT-4o (OpenAI, 2024).

The primary contributions of this paper are as follows:

- We introduce MMathCoT-1M, a synthesized multimodal instruction-tuning dataset that addresses the scarcity of high-quality multimodal mathematical CoT data.
- We propose a novel process-supervised data synthesis method that integrates visual grounding fidelity and logical validity, resulting in DualMath-1.1M, the first

process-supervised dataset for multimodal mathematical reasoning.

- The trained URSA-8B achieves SOTA results on six multimodal mathematics benchmarks among comparable-size MLLMs, establishing a stronger baseline. Additionally, URSA-RM-8B effectively guides multimodal system 2-style reasoning, enabling URSA-8B to surpass GPT-4o while demonstrating out-of-distribution (OOD) generalization capabilities.

2. Related Work

Multimodal Mathematical Reasoning The mathematical reasoning capabilities of MLLMs have recently attracted significant attention (Zhuang et al., 2024; Gao et al., 2023; Li et al., 2024; Dong et al., 2024b; Hu et al., 2024; Yang et al., 2024b; Han et al., 2024; Guo et al., 2024). Unlike traditional mathematical reasoning tasks in Language Models (LLMs) (Luo et al., 2023; Yu et al., 2023), multimodal mathematical reasoning requires MLLMs to interpret visual information and perform cross-modal reasoning between images and text. Tasks such as geometric problem-solving and chart analysis are particularly challenging (Chen et al., 2021). Recent advancements have focused on enhancing visual mathematical inputs through specialized encoders in specific scenarios (Zhang et al., 2024d; Liu et al., 2024a; Chen et al., 2024b). A significant emphasis has also been placed on synthesizing diverse and complex training data. For instance, Math-LLaVA (Shi et al., 2024) introduces the MathV360K dataset, which categorizes images by complexity and enhances associated questions. MultiMath (Peng et al., 2024) curates high-quality reasoning data from K-12 textbooks and employs GPT-4 for CoT data generation and validation. R-CoT (Deng et al., 2024) further diversifies problems through a two-stage reverse question-answer generation process. These data synthesis methods are widely adopted in academia and industry due to their demonstrated efficiency (Sprague et al., 2024; Lu et al., 2023b; Huang et al., 2024; Fu et al., 2024a).

Inference-Time Scaling in Mathematical Reasoning

Recent studies have explored test-time scaling laws in LLMs, aiming to identify optimal reasoning trajectories from diverse thinking trajectories (Zhang et al., 2024b; Gou et al., 2023; Gao et al., 2024; Lin et al., 2024; Zhang et al., 2024a; Kumar et al., 2024; Snell et al., 2024). Initial efforts, such as self-consistency (Wang et al., 2022), have laid the groundwork for test-time scaling. OpenAI has introduced verifiers to supervise and select reasoning paths during inference (Lightman et al., 2023). Math-Shepherd (Wang et al., 2024c) evaluates intermediate reasoning steps based on their likelihood of leading to correct answers, while OmegaPRM (Luo et al., 2024a) constructs Preference Re-

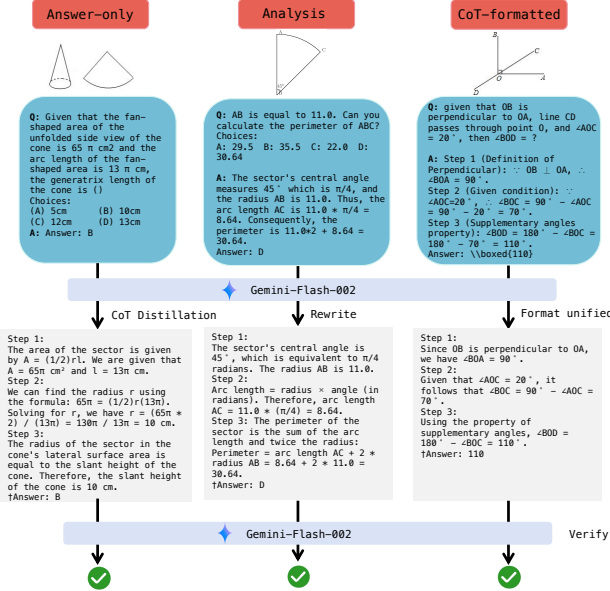


Figure 3: CoT augmentation and verifying for multimodal mathematical data from three type of sources using Gemini-1.5-Flash-002.

ward Model (PRM) training data and employs MCTS for training. Despite these advancements, the lack of models with robust CoT reasoning capabilities and limited exploration into diverse reward model training data remain significant bottlenecks in multimodal mathematical reasoning.

3. Model Training Process

In this section, we introduce the training process of URSA-8B, as illustrated in Figure 5. In Section 3.1, we introduce the model architecture and the composition of the vision-language alignment data. In Section 3.2, we describe the data synthesis strategy for math SFT, named MMathCoT-1M. In Section 3.3, we explain the data synthesis process for training PRM with DualMath-1.1M.

3.1. Vision-Language Alignment

Traditional MLLMs, which are largely trained on tasks like OCR and document understanding for general purposes, are not well-suited for direct transfer to mathematical training (Wang et al., 2024b). In contrast, mathematics-specific LLMs already possess substantial mathematical knowledge and foundational capabilities in mathematical CoT reasoning. Therefore, we choose a composite architecture. We use SAM-B (Kirillov et al., 2023) and SigLIP-L (Zhai et al., 2023) encoders to construct hybrid vision tower (Lu et al., 2024a). On the language model side, we utilize the advanced Qwen2.5-Math-7B-Instruct (Yang et al., 2024a). Following previous work, we use an MLP projector as an aligner between the vision encoder and the LLM (Liu et al., 2024d;

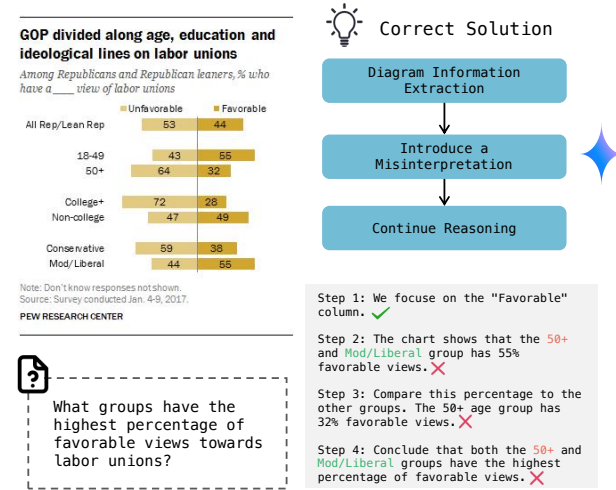


Figure 4: Demonstration of Misinterpretation Insertion Engine.

Bai et al., 2023).

We collect 860K vision-language alignment open-source data for training by combining and filtering open-source datasets, naming it URSA-alignment-860K. The details are listed in Figure 2.

3.2. CoT Augmentation in Multimodal Mathematics

To enhance the multimodal mathematical CoT reasoning capabilities of MLLMs, we collect and categorize existing open-source multimodal mathematical training data. We then employ a generator, Gemini-1.5-Flash-002 (denoted as \mathcal{G}), to synthesize CoT data, as illustrated in Figure 3. Gemini-1.5-Flash-002 demonstrates performance in multimodal mathematical reasoning comparable to GPT-4o while being more cost-effective (Team et al., 2023).

Answer-only Answer-only data $\mathcal{D}_1 = \{(x_i, y_i)\}_{i=1}^{N_1}$ includes MathV360k (Shi et al., 2024), each contains question x_i and ground-truth answer y_i . Answer-only training restricts the model from fully capturing the problem-solving process. It may lead the model to rely on memory-based reasoning, hindering it directly provide answers to more complex reasoning problems through fast thinking (Trinh et al., 2024). Given distillation prompt \mathcal{P}_C , we provide x_i and y_i , then prompt \mathcal{G} to output the reasoning trajectory leading to the answer y_i .

$$\mathcal{S}_{Ao} = \mathcal{G}(\mathcal{P}_C; \{x_i, y_i\}_{i=1}^{N_1}) \quad (1)$$

Analysis-formatted This category, denoted as $\mathcal{D}_2 = \{(x_i, y_i, a_i)\}_{i=1}^{N_2}$, includes datasets such as MAVIS-Geo, MAVIS-MetaGen (Zhang et al., 2024d), VarsityTutors (Zhuang et al., 2024), and Geo170k-QA. Each sam-

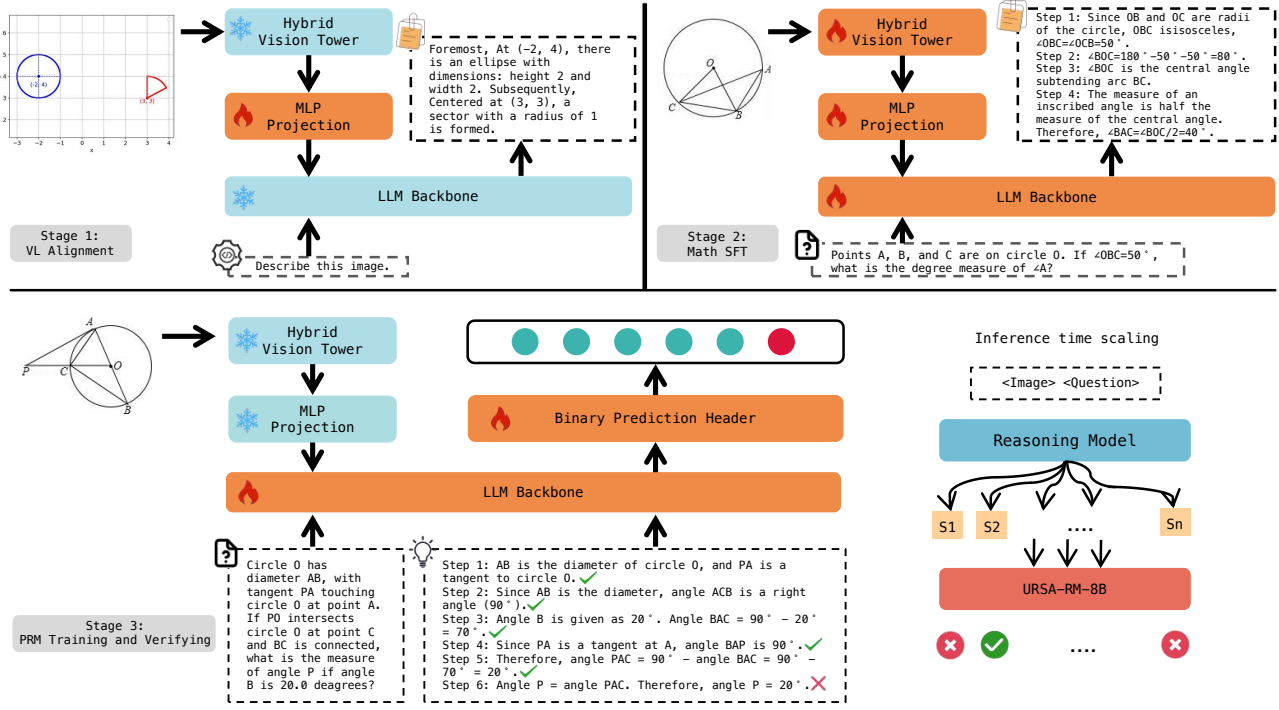


Figure 5: An illustration of the training process for URSA-8B and URSA-RM-8B, with data from the three stages coming from URSA-alignment-860K, MMathCoT-1M, and DualMath-1.1M, respectively. The modules that are frozen and those that need to be trained are distinguished in each stage.

ple contains question x_i , answer y_i and textual analysis a_i . Given rewriting prompt \mathcal{P}_R , we utilize \mathcal{G} to transcribe solutions, enhancing step-by-step reasoning trajectories and linguistic diversity.

$$\mathcal{S}_{An} = \mathcal{G}(\mathcal{P}_R; \{x_i, y_i, a_i\}_{i=1}^{N_2}) \quad (2)$$

CoT-formatted This portion of the data $\mathcal{D}_3 = \{(x_i, y_i, c_i)\}_{i=1}^{N_3}$ is sourced from Multimath300k-en (Peng et al., 2024), each consists of question x_i , answer y_i and CoT solution c_i . We use prompt \mathcal{P}_F and \mathcal{G} to maintain consistency in the CoT output by simply modifying the templates to remove the original design that specified the knowledge points used before the reasoning steps.

$$\mathcal{S}_C = \mathcal{G}(\mathcal{P}_F; \{x_i, y_i, c_i\}_{i=1}^{N_3}) \quad (3)$$

MMathCoT-1M We continue to use \mathcal{G} to perform MLLM-as-a-Judge rejection sampling, filtering out incorrect answers and responses that request additional conditions. Finally, we synthesize a high-quality multimodal mathematical CoT reasoning dataset, MMathCoT-1M, as shown in Equation 4.

$$\mathcal{D}_{SFT} = \{(x_i, y_i) \sim \mathcal{S}_{Ao} \cup \mathcal{S}_{An} \cup \mathcal{S}_C\}_{i=1}^{|\mathcal{S}_{Ao} \cup \mathcal{S}_{An} \cup \mathcal{S}_C|} \quad (4)$$

We use instruction fine-tuning to train URSA-8B based on the aligned model proposed in Section 3.1. Training loss is

displayed in Equation 5.

$$\mathcal{L}_{SFT} = -\mathbb{E}_{(x,y) \sim \mathcal{D}_{SFT}} \sum_{t=1}^T \log \mathcal{M}(y_t | x, y_{:t}) \quad (5)$$

We provide prompts for three types of data processing in Appendix D.1.

3.3. Dual-view Process Supervised Data Synthesis

However, even though URSA-8B possesses strong CoT reasoning capabilities, it still has a significant likelihood of producing incorrect reasoning trajectories. Inspired by the use of process supervision for test-time scaling in LLM reasoning (Zhang et al., 2024b; Setlur et al., 2024; Zelikman et al., 2022), we consider training a multimodal process supervision model to extract high-quality CoT trajectories. In multimodal scenarios, we propose a dual-view process reward data approach, focusing on both “logically correct” and “visually accurate” aspects. The former is derived from error localization in the incorrect reasoning trajectories of URSA-8B, while the latter comes from manually inserted image misinterpretations.

Error Step Locating Engine Inspired by (Lightman et al., 2023; Luo et al., 2024a), the Monte Carlo Tree Search (MCTS) approach can help us identify erroneous steps in

Algorithm 1 BinaryErrorLocating

Input: Negative example set $Y_n = \{y_i^n | i = 1, 2, \dots, N\}$, mid step sampling num N_{mid} .
ErrorLocatingSet $\leftarrow []$
for $i = 1$ **to** N **do**
 $l \leftarrow 0$, $r \leftarrow \text{StepLen}(y_i^n)$
 while $l < r$ **do**
 $\text{mid} \leftarrow (l + r) // 2$
 $\text{MID_RES} \leftarrow \text{Generate}([y_{i,1}^n, y_{i,2}^n, \dots, y_{i,mid}^n], N_{mid})$
 if True not in $\text{Verify}(\text{MID_RES})$ **then**
 $r \leftarrow \text{mid}$
 else
 $l \leftarrow \text{mid} + 1$
 end if
 end while
 $e_i^n \leftarrow \text{WrongStepLabeling}(y_i^n, l)$
 $\text{ErrorLocatingSet.append}(e_i^n)$
end for
Output: ErrorLocatingSet

the trajectory of problem-solving. We use the binary labeling approach to mark erroneous steps, enabling automated generation of process reward signals.

Given positive and negative solution pairs $\{y_i^p, y_i^n\}_{i=1}^N$, We obtain the positive example set $Y_p = \{y_i^p | i = 1, 2, \dots, N\}$ and negative example set $Y_n = \{y_i^n | i = 1, 2, \dots, N\}$. For the positive example set Y_p , we directly perform forward labeling on each step of all samples. For the negative example set Y_n , we execute the *BinaryErrorLocating* operation.

$$\mathcal{S}_{BEL} = \text{BinaryErrorLocating}(Y_n, N_{mid}) \quad (6)$$

In the experiment, we set $N_{mid} = 16$ in Equation 6.

Misinterpretation Insertion Engine The reward signals generated by MCTS come from the logical correctness of the text modality, without giving special attention to the uniqueness of image and text fusion. Some previous works have also suggested that MLLMs exhibit a considerable degree of misunderstanding of visual signals (Yan et al., 2024; Zheng et al., 2024) during reasoning. Therefore, we consider a misinterpreting insertion technique to construct training data for visual information attention.

As shown in Figure 4, the misinterpretation insertion engine involves three stages. In the **first stage**, the model extracts mathematical paradigm information from image. In the **second stage**, the model is prompted to identify potential misinterpretations within the correct solution. In the **third stage**, the model selects information to misinterpret, injects it, and continues the reasoning process to arrive at an incorrect trajectory. Finally, we obtain \mathcal{S}_{MIE} .

By using two engines, we obtain 1.1M process-supervised

training data named DualMath-1.1M. We continue training on URSA-8B with a binary classification loss shown in Equation 8 to obtain URSA-RM-8B. \mathcal{M}_p is the trained URSA-RM-8B.

$$\mathcal{D}_{PRM} = \{(e_i, y_{e_i}) \sim \mathcal{S}_{BEL} \cup \mathcal{S}_{MIE}\} \quad (7)$$

$$\begin{aligned} \mathcal{L}_{PRM} = -\mathbb{E}_{(e,y) \sim \mathcal{D}_{PRM}} \sum_{j=1}^{|e|} & \left[y_j \log \mathcal{M}_p(e_j) \right. \\ & \left. + (1 - y_j) \log(1 - \mathcal{M}_p(e_j)) \right] \end{aligned} \quad (8)$$

4. Experiment

4.1. Experimental Setup

Benchmarks We evaluate URSA-8B on six widely used benchmarks, including MathVista (Lu et al., 2023a), MathVerse (Zhang et al., 2025), DYNAMATH (Zou et al., 2024), WE-MATH (Qiao et al., 2024), GeoQA (Chen et al., 2021) and MathVision (Wang et al., 2024c). Dataset metrics are detailed in Appendix E. We consistently employ zero-shot reasoning.

Baselines We select closed-source MLLMs, open-source general MLLMs, and open-source MLLMs specifically optimized for mathematical reasoning as baselines for a comprehensive comparison. Specifically, for general MLLMs, we choose very powerful models like Qwen2-VL and InterVL2.5-8B as baselines. For math MLLMs, we select most recent works such as Math-PUMA, Multimath and InfiMM-Math.

Implementation Details Our experiments are based on Python 3.10 and PyTorch 2.4.0+cu124. We use AdamW (Diederik, 2014) as the optimizer. For the three stages, the learning rates are set to 1e-4, 1e-5, and 5e-6, respectively, with a warm-up ratio maintained at 0.02. The training epochs are 1, 2, and 2. We use Fully Shared Data Parallel (FSDP) as the distributed training framework. By default, our experiments are conducted using 32 × NVIDIA-H100-HBM3 devices. A more detailed experiment setup and time costs are shown in Appendix A.

4.2. Main Results

Results of URSA-8B We evaluate the URSA-8B model on MathVerse, MathVista, and DYNAMATH, achieving SOTA performance across multiple metrics among open-source MLLMs. As shown in Table 1, URSA-8B excels in both overall performance and math-specific tasks on MathVista, outperforming strong open-source models such as Qwen2-VL and InternVL2-8B. Specifically, URSA-8B surpasses the second-best math MLLMs by 12.5 and 7.0 percentage points in the math-related tasks GPS and MWP, re-

Table 1: Comparison with closed-source MLLMs and open-source MLLMs on **MATHVISTA testmini** and **MATHVERSE testmini**. The best is **bold**, and the runner-up is underline. The best results of Closed-source MLLMs are highlighted in green. The best and second-best results of Open-source MLLMs are highlighted in red and blue respectively.

Model	#Params	MathVista							MathVerse						
		ALL	GPS	MWP	FQA	TQA	VQA	ALL	TD	TL	TO	VI	VD	VO	
<i>Baselines</i>															
Random	-	17.9	21.6	3.8	18.2	19.6	26.3	12.4	12.4	12.4	12.4	12.4	12.4	12.4	12.4
Human	-	60.3	48.4	73.0	59.7	63.2	55.9	64.9	71.2	70.9	41.7	61.4	68.3	66.7	
<i>Closed-Source MLLMs</i>															
GPT-4o (OpenAI, 2024)	-	63.8	64.7	-	-	-	-	50.8	59.8	50.3	52.4	48.0	46.5	47.6	
GPT-4V (OpenAI, 2023)	-	49.9	50.5	57.5	43.1	65.2	38.0	39.4	54.7	41.4	48.7	34.9	34.4	31.6	
Gemini-1.5-Flash-002 (Team et al., 2023)	-	58.4	-	-	-	-	-	49.4	57.2	50.5	50.3	47.6	45.1	45.4	
Gemini-1.5-Pro (Team et al., 2023)	-	63.9	-	-	-	-	-	35.3	39.8	34.7	44.5	32.0	36.8	33.3	
Claude-3.5-Sonnet (Anthropic, 2024)	-	67.7	-	-	-	-	-	-	-	-	-	-	-	-	
Qwen-VL-Plus (Bai et al., 2023)	-	43.3	35.5	31.2	54.6	48.1	51.4	21.3	26.0	21.2	25.2	18.5	19.1	21.8	
<i>Open-Source General MLLMs</i>															
mPLUG-Owl2-7B (Ye et al., 2023)	7B	22.2	23.6	10.2	22.7	27.2	27.9	10.3	11.6	11.4	13.8	11.1	9.4	8.0	
MiniGPT4-7B (Zhu et al., 2023)	7B	23.1	26.0	13.4	18.6	30.4	30.2	12.2	12.3	12.9	13.4	12.5	14.8	8.7	
LLaVA-1.5-13B (Liu et al., 2024b)	13B	27.7	22.7	18.9	23.8	43.0	30.2	12.7	17.1	12.0	22.6	12.6	12.7	9.0	
SPHINX-V2-13B (Lin et al., 2023)	13B	36.7	16.4	23.1	54.6	41.8	43.0	16.1	20.8	14.1	14.0	16.4	15.6	16.2	
LLaVA-NeXT-34B (Liu et al., 2024c)	34B	46.5	-	-	-	-	-	34.6	49.0	37.6	30.1	35.2	28.9	22.4	
InternLM-XComposer2-VL (Dong et al., 2024a)	7B	57.6	63.0	73.7	55.0	56.3	39.7	25.9	36.9	28.3	42.5	20.1	24.4	19.8	
Deepseek-VL (Lu et al., 2024a)	8B	34.9	28.4	55.9	26.8	32.9	34.6	19.3	23.0	23.2	23.1	20.2	18.4	11.8	
LLaVA-OneVision (SI) (Li et al., 2024)	8B	58.6	71.6	69.4	51.3	56.3	45.3	-	-	-	-	-	-	26.9	
Qwen2-VL (Wang et al., 2024b)	8B	58.9	40.9	64.0	69.1	60.1	58.1	33.6	37.4	33.5	35.0	31.3	30.3	28.1	
InternVL2-8B (Chen et al., 2024c)	8B	58.3	62.0	59.1	58.7	61.4	49.7	35.9	39.0	33.8	36.0	32.2	30.9	27.7	
InternVL2.5-8B (Chen et al., 2024a)	8B	64.5	64.9	70.4	63.2	66.5	58.1	-	-	-	-	-	-	22.8	
<i>Open-Source Math MLLMs</i>															
G-LLaVA-7B (Gao et al., 2023)	7B	25.1	48.7	3.6	19.1	25.0	28.7	16.6	20.9	20.7	21.1	17.2	14.6	9.4	
Math-LLaVA-13B (Shi et al., 2024)	13B	46.6	57.7	56.5	37.2	51.3	33.5	22.9	27.3	24.9	27.0	24.5	21.7	16.1	
Math-PUMA-Qwen2-7B (Zhuang et al., 2024)	8B	47.9	48.1	68.3	46.5	46.2	30.2	33.6	42.1	35.0	39.8	33.4	31.6	26.0	
Math-PUMA-DeepSeek-Math (Zhuang et al., 2024)	7B	44.7	39.9	67.7	42.8	42.4	31.3	31.8	43.4	35.4	47.5	33.6	31.6	14.7	
MAVIS-7B (Zhang et al., 2024d)	7B	-	64.1	-	-	-	-	35.2	43.2	37.2	-	34.1	29.7	31.8	
InfiMM-Math (Han et al., 2024)	7B	-	-	-	-	-	-	34.5	46.7	32.4	-	38.1	32.4	15.8	
Multimath-7B (Peng et al., 2024)	7B	50.0	66.8	61.8	40.1	50.0	33.0	27.7	34.8	30.8	35.3	28.1	25.9	15.0	
URSA-8B	8B	59.8	79.3	75.3	44.6	63.9	40.2	45.7	55.3	48.3	51.8	46.4	43.9	28.6	
Δ over SOTA Open-Source Math MLLMs	-	+9.8	+12.5	+7.0	-1.9	+12.6	+6.7	+10.5	+8.6	+11.1	+4.3	+8.3	+11.5	-3.2	

spectively. However, similar to other math MLLMs, URSA-8B underperforms on FQA and VQA due to a lack of specialized focus on these tasks. On the MathVerse benchmark, URSA-8B demonstrates comprehensive improvements compared to general MLLMs, with particularly notable advantages in the Vision-Intensive and Vision-Dominant subsets, whereas previous math MLLMs showed minimal performance gaps. It highlights the universal benefits of enhanced CoT reasoning without trade-offs from modality imbalances. URSA-8B shows slightly lower performance in Vision-Only tasks compared to MAVIS-7B, which incorporates mathematical knowledge enhancements into its vision encoder.

The results of URSA-8B on the WE-MATH dataset are shown in Table 2. Among the performances of closed-source models, URSA-8B has surpassed GPT-4V in average performance, IK, and CM, and has almost entirely outperformed Gemini-1.5-Pro, with only some gap remaining compared to GPT-4o. When compared to open-source general MLLMs and open-source math MLLMs, URSA-8B has almost completely surpassed the current SOTA models Qwen2-VL and Math-PUMA in both strict and loose settings, showing a

significant advantage.

In addition, we use DYNAMATH to help verify the robustness of URSA-8B’s reasoning capabilities. As shown in Table 3, URSA-8B demonstrates superior performance on DYNAMATH compared to Qwen2-VL and InternVL2-8B, showing significant advantages in the Plane Geometry and Algebra subsets. This further confirms the benefits of enhancing the model’s CoT reasoning capabilities in terms of generalization. The results on GeoQA and Math-Vision are demonstrated in Appendix C.2 and Appendix C.3.

System 2-style Performance In Figure 6, we show the pass@N performance of URSA-8B. With only 4 time sampling, URSA-8B can achieve a pass rate of 90.9 on the GPS task of Mathvista. The pass@64 performance on MathVista is 97.1, indicating that URSA-8B already has substantial coverage of geometric problem-solving strategies. On MathVerse and Math-Vision datasets, URSA-8B also demonstrates a high upper limit of reasoning capability. Furthermore, when paired with URSA-RM-8B as a verifier, the accuracy significantly surpasses that of self-consistency,

Table 2: The performance comparison with Closed-source MLLMs and Open-source MLLMs on four-dimensional metrics for **WE-MATH testmini** reasoning evaluation. The best results of Closed-source MLLMs are highlighted in green. The best and second-best results of Open-source MLLMs are highlighted in red and blue respectively.

Model	#Params	Strict					Loose				
		AVG ↑	IK ↓	IG ↓	CM ↑	RM ↓	AVG ↑	IK ↓	IG ↓	CM ↑	RM ↓
<i>Closed-source MLLMs</i>											
Qwen-VL-Max (Bai et al., 2023)	-	10.5	65.1	7.6	6.7	75.5	25.5	65.1	7.6	21.7	20.3
Gemini-1.5-Pro (Team et al., 2023)	-	26.4	42.9	11.2	20.8	54.8	46.0	42.9	11.2	40.4	12.0
GPT-4V (OpenAI, 2023)	-	31.1	39.8	14.5	23.8	47.9	51.4	39.8	14.5	44.2	3.3
GPT-4o (OpenAI, 2024)	-	42.9	31.2	15.2	35.2	34.2	60.6	31.2	15.2	53.0	1.1
<i>Open-source General MLLMs</i>											
LLaVA-1.6 (Liu et al., 2024c)	7B	3.3	78.3	2.5	2.1	89.1	13.8	78.3	2.5	12.6	34.7
LLaVA-1.6 (Liu et al., 2024c)	13B	5.2	69.1	3.2	3.6	86.9	22.0	69.1	3.2	20.4	26.2
InternVL-Chat-V1.5 (Chen et al., 2024b)	26B	12.7	56.4	10.5	7.4	77.6	31.0	56.4	10.5	25.7	22.4
LLaVA-NeXT (Liu et al., 2024c)	72B	13.4	58.9	7.1	9.9	71.0	31.5	58.9	7.1	28.0	17.9
DeepSeek-VL (Lu et al., 2024a)	8B	6.3	69.1	4.6	4.0	84.8	21.0	69.1	4.6	18.7	29.0
Phi3-Vision (Abdin et al., 2024)	4.2B	10.6	58.9	9.0	6.1	81.1	29.8	58.9	9.0	25.3	21.3
GLM-4V-9B (GLM et al., 2024)	9B	14.9	53.0	9.5	10.1	73.1	35.1	53.0	9.5	30.3	19.3
InternLM-XComposer2-VL (Dong et al., 2024a)	7B	12.7	56.4	10.5	7.4	77.6	31.0	56.4	10.5	25.7	22.4
LLaVA-OneVision (Li et al., 2024)	8B	23.1	45.0	13.1	16.6	60.5	44.9	45.0	13.1	38.3	8.6
InternVL2-8B (Chen et al., 2024c)	8B	26.6	45.5	13.5	19.8	51.6	44.9	45.5	13.5	38.1	7.0
Qwen2-VL (Wang et al., 2024b)	8B	25.6	47.1	14.7	18.3	52.2	43.0	47.1	14.7	35.6	7.0
<i>Open-source Math MLLMs</i>											
G-LLaVA (Gao et al., 2023)	13B	6.5	64.2	4.6	4.2	86.6	22.3	64.2	4.6	20.0	36.0
Math-LLaVA (Shi et al., 2024)	13B	11.1	62.1	3.6	9.3	72.8	31.3	62.1	3.6	29.5	13.9
Math-PUMA-Qwen2-7B (Zhuang et al., 2024)	8B	19.2	47.8	13.7	12.4	67.8	41.0	47.8	13.7	34.1	11.4
Math-PUMA-DeepSeek-Math-7B (Zhuang et al., 2024)	7B	15.6	56.0	7.2	12.0	67.4	35.8	56.0	7.2	32.2	12.4
InfiMM-Math (Han et al., 2024)	7B	20.6	48.8	12.2	15.2	61.7	-	-	-	-	-
URSA-8B	8B	32.2	37.5	10.7	26.9	48.2	53.5	37.5	10.7	48.2	7.0
Δ over SOTA <i>Open-Source Math MLLMs</i>	-	+11.6	+10.3	-7.1	+11.7	+13.5	+12.5	+10.3	-7.1	+14.1	+4.4

Table 3: Comparison with open-source MLLMs on **DYNA-MATH testmini** dataset.

Model	ALL	PG	SG	AG	AL	PT	GT	AR
<i>Closed-source MLLMs</i>								
GPT-4o	63.7	56.8	52.0	61.0	76.9	51.8	58.1	61.5
Claude-3.5-Sonnet	64.8	49.9	49.3	55.3	81.0	44.1	69.4	61.2
Geimini-1.5-Pro	60.5	52.7	42.7	61.6	70.8	20.6	65.2	54.2
<i>Open-source MLLMs</i>								
Llava-v1.5-7B	16.6	10.5	7.3	19.5	6.5	8.2	32.3	10.8
Llava-v1.6-34B	27.1	21.4	25.3	27.6	14.9	7.6	32.7	23.1
Deepseek-VL-7B-chat	21.5	16.0	13.3	26.5	12.9	4.7	32.3	12.7
InternVL2-8B	39.7	33.9	37.3	32.5	46.9	15.9	42.1	37.3
Qwen2-VL	42.1	40.3	38.7	39.9	37.1	8.2	44.8	39.2
URSA-8B	44.7	48.1	38.0	33.7	66.9	24.7	39.2	38.5

making it a superior tool for test-time scaling in multimodal mathematical reasoning. Notably, on the more challenging Math-Vision benchmark, employing system-2 reasoning with URSA-RM-8B and a sampling count of 8 surpasses the performance of GPT-4o (32.6 vs. 30.4). We also compare the pass@N of Multimath-7B and find that URSA-8B has a significantly higher upper limit in reasoning performance than Multimath-7B. On MathVerse, the pass@64 of URSA-8B shows a relative improvement of 74.2% compared to single inference, while Multimath-7B only shows

Table 4: OOD performance when URSA-RM-8B works on Multimath-7B.

Method	Sampling Number				
	N=4	N=8	N=16	N=32	N=64
<i>MathVista-GPS</i>					
Self-Consistency	67.4	67.9	68.2	68.7	68.9
URSA-RM-8B	68.8	69.7	70.4	70.7	70.8
<i>MathVerse</i>					
Self-Consistency	29.1	29.7	30.1	30.2	30.2
URSA-RM-8B	31.0	32.7	33.0	33.2	33.0

an improvement of 58.5%. This further demonstrates the role of training with high-quality CoT reasoning data in enhancing reasoning capabilities and raising the upper limit of test-time scaling benefits.

Additionally, we test whether URSA-RM-8B can fulfill the role of an OOD verifier. We choose Multimath as the base model, as it is relatively stable in performing CoT solutions after mathematics instruction tuning. As shown in the results of Table 4, we find that URSA-RM-8B effectively serves as a verifier for Multimath’s CoT solutions, surpassing the performance of self-consistency.

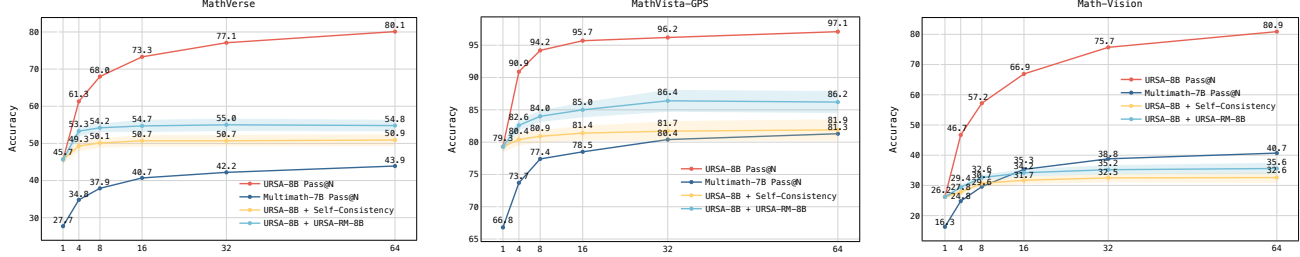


Figure 6: Pass@N and Best-of-N results comparison on MathVerse, MathVista-GPS and Math-Vision.

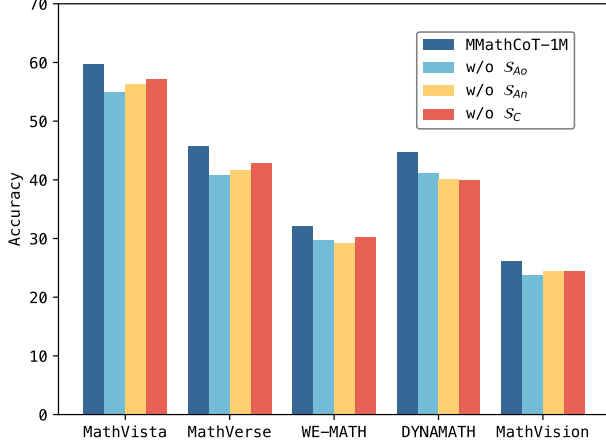


Figure 7: Ablation study with respect to MMathCoT-1M during the Math SFT stage on all used benchmarks. 'w/o S' means replacing the set with the original data, allowing us to maintain the total number of SFT data.

Table 5: Ablation study on URSA-RM-8B.

Method	Sampling Number				
	N=4	N=8	N=16	N=32	N=64
<i>MathVista-GPS</i>					
URSA-RM-8B	82.6	84.0	85.0	86.4	86.2
URSA-RM-8B w/o S_{BEL}	80.1	81.7	82.2	83.1	83.0
URSA-RM-8B w/o S_{MIE}	81.3	82.8	83.1	83.5	83.6
<i>MathVerse</i>					
URSA-RM-8B	53.2	54.2	54.7	55.0	54.8
URSA-RM-8B w/o S_{BEL}	49.9	50.7	51.8	52.0	52.1
URSA-RM-8B w/o S_{MIE}	50.8	51.6	52.4	52.9	53.1

5. Ablations

5.1. Ablation on CoT Data Synthesis

In Figure 7, we demonstrate the effectiveness of various data synthesis strategies. Firstly, it is shown across all datasets that using the complete synthesized data achieves the best results, highlighting the role of MMathCoT-1M data. More specifically, we find: i) S_{AO} demonstrates the greatest impact on MathVista, MathVerse, and MathVision, indicating that distilled CoT data is important for problems where

absolute solution accuracy is pursued; ii) However, on WE-MATH, the replacement of S_{An} leads to the most significant performance drop, suggesting that content rewriting better aligns with the end-to-end requirements posed by the WE-MATH benchmark, and mixing training with data lacking clear logical sequences may reduce hierarchical accuracy; iii) The results on DYNAMATH indicate that rewriting and natural language formulation effectively enhance reasoning robustness from the perspective of textual diversity.

5.2. Ablation on PRM Training Data Synthesis

We conduct an ablation study on synthetic data for URSA-RM-8B to verify the effectiveness of error step locating engine and misinterpretation insertion engine, respectively. We validate this on MathVerse and MathVista-GPS, and the results are shown in Table 5. Removing any single component individually leads to a decline in Best-of-N performance on both benchmarks, indicating that verifying from both logical errors and image-text matching relationships are effective data synthesis strategies. The limitation of the latter lies in designing different prompts for different types of problems, making it somewhat distribution-specific.

6. Conclusion

In this work, we enhance the mathematical reasoning capabilities of MLLMs by proposing a streamlined training approach, from high-quality CoT fine-tuning to multimodal math test-time scaling. To address the lack of high-quality reasoning processes in existing datasets, we introduce MMathCoT-1M, a refined mathematics CoT training dataset created through CoT distillation, rewriting, and style unification. Using this 1M-size dataset, we train URSA-8B, which achieves SOTA results on major benchmarks. Additionally, we extend our focus to improving CoT supervision by developing DualMath-1.1M, a dual-view supervised synthetic dataset, and training URSA-RM-8B as a verifier. URSA-RM-8B effectively enhances URSA-8B's reasoning abilities and demonstrates strong performance in OOD scenarios. This work bridges the gap between high-quality CoT fine-tuning and System 2-style reasoning in multimodal mathematics, laying a robust foundation for future research in critic-based or reinforcement learning applications.

References

Abdin, M., Aneja, J., Awadalla, H., Awadallah, A., Awan, A. A., Bach, N., Bahree, A., Bakhtiari, A., Bao, J., Behl, H., et al. Phi-3 technical report: A highly capable language model locally on your phone. *arXiv preprint arXiv:2404.14219*, 2024.

An, S., Zhou, B., Lin, Z., Fu, Q., Chen, B., Zheng, N., Chen, W., and Lou, J.-G. Skill-based few-shot selection for in-context learning. In *Proceedings of the 2023 Conference on Empirical Methods in Natural Language Processing*, pp. 13472–13492, 2023.

Anthropic. The claude 3 model family: Opus, sonnet, haiku. <https://www.anthropic.com/claude-3-model-card>, 2024. Claude-3 Model Card.

Bai, J., Bai, S., Yang, S., Wang, S., Tan, S., Wang, P., Lin, J., Zhou, C., and Zhou, J. Qwen-vl: A versatile vision-language model for understanding, localization, text reading, and beyond. *arXiv preprint arXiv:2308.12966*, 1(2): 3, 2023.

Browne, C. B., Powley, E., Whitehouse, D., Lucas, S. M., Cowling, P. I., Rohlfsagen, P., Tavener, S., Perez, D., Samothrakis, S., and Colton, S. A survey of monte carlo tree search methods. *IEEE Transactions on Computational Intelligence and AI in games*, 4(1):1–43, 2012.

Chen, J., Tang, J., Qin, J., Liang, X., Liu, L., Xing, E., and Lin, L. Geoqa: A geometric question answering benchmark towards multimodal numerical reasoning. In *Findings of the Association for Computational Linguistics: ACL-IJCNLP 2021*, pp. 513–523, 2021.

Chen, J., Li, D. Z. X. S. X., Zhang, Z. L. P., Xiong, R. K. V. C. Y., and Elhoseiny, M. Minigpt-v2: Large language model as a unified interface for vision-language multi-task learning. *arXiv preprint arXiv:2310.09478*, 2023.

Chen, Z., Wang, W., Cao, Y., Liu, Y., Gao, Z., Cui, E., Zhu, J., Ye, S., Tian, H., Liu, Z., et al. Expanding performance boundaries of open-source multimodal models with model, data, and test-time scaling. *arXiv preprint arXiv:2412.05271*, 2024a.

Chen, Z., Wang, W., Tian, H., Ye, S., Gao, Z., Cui, E., Tong, W., Hu, K., Luo, J., Ma, Z., et al. How far are we to gpt-4v? closing the gap to commercial multimodal models with open-source suites. *arXiv preprint arXiv:2404.16821*, 2024b.

Chen, Z., Wu, J., Wang, W., Su, W., Chen, G., Xing, S., Zhong, M., Zhang, Q., Zhu, X., Lu, L., et al. Internvl: Scaling up vision foundation models and aligning for generic visual-linguistic tasks. In *Proceedings of the IEEE/CVF Conference on Computer Vision and Pattern Recognition*, pp. 24185–24198, 2024c.

Chu, Z., Chen, J., Chen, Q., Yu, W., He, T., Wang, H., Peng, W., Liu, M., Qin, B., and Liu, T. A survey of chain of thought reasoning: Advances, frontiers and future. *arXiv preprint arXiv:2309.15402*, 2023.

Deng, L., Liu, Y., Li, B., Luo, D., Wu, L., Zhang, C., Lyu, P., Zhang, Z., Zhang, G., Ding, E., et al. R-cot: Reverse chain-of-thought problem generation for geometric reasoning in large multimodal models. *arXiv preprint arXiv:2410.17885*, 2024.

Diederik, P. K. Adam: A method for stochastic optimization. *(No Title)*, 2014.

Dong, X., Zhang, P., Zang, Y., Cao, Y., Wang, B., Ouyang, L., Wei, X., Zhang, S., Duan, H., Cao, M., et al. Internlm-xcomposer2: Mastering free-form text-image composition and comprehension in vision-language large model. *arXiv preprint arXiv:2401.16420*, 2024a.

Dong, Y., Liu, Z., Sun, H.-L., Yang, J., Hu, W., Rao, Y., and Liu, Z. Insight-v: Exploring long-chain visual reasoning with multimodal large language models. *arXiv preprint arXiv:2411.14432*, 2024b.

Fu, C., Lin, H., Long, Z., Shen, Y., Zhao, M., Zhang, Y., Dong, S., Wang, X., Yin, D., Ma, L., et al. Vita: Towards open-source interactive omni multimodal llm. *arXiv preprint arXiv:2408.05211*, 2024a.

Fu, D., Xiao, T., Wang, R., Zhu, W., Zhang, P., Pang, G., Jia, R., and Chen, L. Tldr: Token-level detective reward model for large vision language models. *arXiv preprint arXiv:2410.04734*, 2024b.

Gao, B., Cai, Z., Xu, R., Wang, P., Zheng, C., Lin, R., Lu, K., Lin, J., Zhou, C., Xiao, W., et al. Llm critics help catch bugs in mathematics: Towards a better mathematical verifier with natural language feedback. *CoRR*, 2024.

Gao, J., Pi, R., Zhang, J., Ye, J., Zhong, W., Wang, Y., Hong, L., Han, J., Xu, H., Li, Z., et al. G-llava: Solving geometric problem with multi-modal large language model. *arXiv preprint arXiv:2312.11370*, 2023.

GLM, T., Zeng, A., Xu, B., Wang, B., Zhang, C., Yin, D., Rojas, D., Feng, G., Zhao, H., Lai, H., Yu, H., Wang, H., Sun, J., Zhang, J., Cheng, J., Gui, J., Tang, J., Zhang, J., Li, J., Zhao, L., Wu, L., Zhong, L., Liu, M., Huang, M., Zhang, P., Zheng, Q., Lu, R., Duan, S., Zhang, S., Cao, S., Yang, S., Tam, W. L., Zhao, W., Liu, X., Xia, X., Zhang, X., Gu, X., Lv, X., Liu, X., Liu, X., Yang, X., Song, X., Zhang, X., An, Y., Xu, Y., Niu, Y., Yang, Y., Li, Y., Bai, Y., Dong, Y., Qi, Z., Wang, Z., Yang, Z., Du, Z., Hou, Z., and Wang, Z. Chatglm: A family of large language models from glm-130b to glm-4 all tools, 2024.

Gou, Z., Shao, Z., Gong, Y., Shen, Y., Yang, Y., Duan, N., and Chen, W. Critic: Large language models can self-correct with tool-interactive critiquing. *arXiv preprint arXiv:2305.11738*, 2023.

Guo, J., Zheng, T., Bai, Y., Li, B., Wang, Y., Zhu, K., Li, Y., Neubig, G., Chen, W., and Yue, X. Mammoth-vl: Eliciting multimodal reasoning with instruction tuning at scale. *arXiv preprint arXiv:2412.05237*, 2024.

Han, X., Jian, Y., Hu, X., Liu, H., Wang, Y., Fan, Q., Ai, Y., Huang, H., He, R., Yang, Z., et al. Infimm-webmath-40b: Advancing multimodal pre-training for enhanced mathematical reasoning. In *The 4th Workshop on Mathematical Reasoning and AI at NeurIPS'24*, 2024.

Hu, Y., Shi, W., Fu, X., Roth, D., Ostendorf, M., Zettlemoyer, L., Smith, N. A., and Krishna, R. Visual sketchpad: Sketching as a visual chain of thought for multimodal language models. *arXiv preprint arXiv:2406.09403*, 2024.

Huang, Y., Liu, X., Gong, Y., Gou, Z., Shen, Y., Duan, N., and Chen, W. Key-point-driven data synthesis with its enhancement on mathematical reasoning. *arXiv preprint arXiv:2403.02333*, 2024.

Kirillov, A., Mintun, E., Ravi, N., Mao, H., Rolland, C., Gustafson, L., Xiao, T., Whitehead, S., Berg, A. C., Lo, W.-Y., et al. Segment anything. In *Proceedings of the IEEE/CVF International Conference on Computer Vision*, pp. 4015–4026, 2023.

Kumar, A., Zhuang, V., Agarwal, R., Su, Y., Co-Reyes, J. D., Singh, A., Baumli, K., Iqbal, S., Bishop, C., Roelofs, R., et al. Training language models to self-correct via reinforcement learning. *arXiv preprint arXiv:2409.12917*, 2024.

Kwon, W., Li, Z., Zhuang, S., Sheng, Y., Zheng, L., Yu, C. H., Gonzalez, J., Zhang, H., and Stoica, I. Efficient memory management for large language model serving with pagedattention. In *Proceedings of the 29th Symposium on Operating Systems Principles*, pp. 611–626, 2023.

Li, B., Zhang, Y., Guo, D., Zhang, R., Li, F., Zhang, H., Zhang, K., Zhang, P., Li, Y., Liu, Z., et al. Llava-onevision: Easy visual task transfer. *arXiv preprint arXiv:2408.03326*, 2024.

Liang, Z., Yang, T., Zhang, J., and Zhang, X. Unimath: A foundational and multimodal mathematical reasoner. In *Proceedings of the 2023 Conference on Empirical Methods in Natural Language Processing*, pp. 7126–7133, 2023.

Liang, Z., Liu, Y., Niu, T., Zhang, X., Zhou, Y., and Yavuz, S. Improving llm reasoning through scaling inference computation with collaborative verification. *arXiv preprint arXiv:2410.05318*, 2024.

Lightman, H., Kosaraju, V., Burda, Y., Edwards, H., Baker, B., Lee, T., Leike, J., Schulman, J., Sutskever, I., and Cobbe, K. Let's verify step by step. *arXiv preprint arXiv:2305.20050*, 2023.

Lin, Z., Liu, C., Zhang, R., Gao, P., Qiu, L., Xiao, H., Qiu, H., Lin, C., Shao, W., Chen, K., et al. Sphinx: The joint mixing of weights, tasks, and visual embeddings for multi-modal large language models. *arXiv preprint arXiv:2311.07575*, 2023.

Lin, Z., Gou, Z., Liang, T., Luo, R., Liu, H., and Yang, Y. CriticBench: Benchmarking LLMs for critique-correct reasoning. In Ku, L.-W., Martins, A., and Srikumar, V. (eds.), *Findings of the Association for Computational Linguistics: ACL 2024*, pp. 1552–1587, Bangkok, Thailand, August 2024. Association for Computational Linguistics. doi: 10.18653/v1/2024.findings-acl.91. URL <https://aclanthology.org/2024.findings-acl.91>.

Liu, D., Zhang, R., Qiu, L., Huang, S., Lin, W., Zhao, S., Geng, S., Lin, Z., Jin, P., Zhang, K., et al. Sphinx-x: Scaling data and parameters for a family of multi-modal large language models. *arXiv preprint arXiv:2402.05935*, 2024a.

Liu, H., Li, C., Li, Y., and Lee, Y. J. Improved baselines with visual instruction tuning. In *Proceedings of the IEEE/CVF Conference on Computer Vision and Pattern Recognition*, pp. 26296–26306, 2024b.

Liu, H., Li, C., Li, Y., Li, B., Zhang, Y., Shen, S., and Lee, Y. J. Llava-next: Improved reasoning, ocr, and world knowledge, 2024c.

Liu, H., Li, C., Wu, Q., and Lee, Y. J. Visual instruction tuning. *Advances in neural information processing systems*, 36, 2024d.

Lu, H., Liu, W., Zhang, B., Wang, B., Dong, K., Liu, B., Sun, J., Ren, T., Li, Z., Yang, H., et al. Deepseek-vl: towards real-world vision-language understanding. *arXiv preprint arXiv:2403.05525*, 2024a.

Lu, P., Bansal, H., Xia, T., Liu, J., Li, C., Hajishirzi, H., Cheng, H., Chang, K.-W., Galley, M., and Gao, J. Mathvista: Evaluating mathematical reasoning of foundation models in visual contexts. *arXiv preprint arXiv:2310.02255*, 2023a.

Lu, S., Li, Y., Chen, Q.-G., Xu, Z., Luo, W., Zhang, K., and Ye, H.-J. Ovis: Structural embedding alignment for multimodal large language model. *arXiv preprint arXiv:2405.20797*, 2024b.

Lu, Y., Shen, M., Wang, H., Wang, X., van Rechem, C., Fu, T., and Wei, W. Machine learning for synthetic data generation: a review. *arXiv preprint arXiv:2302.04062*, 2023b.

Luo, H., Sun, Q., Xu, C., Zhao, P., Lou, J., Tao, C., Geng, X., Lin, Q., Chen, S., and Zhang, D. Wizardmath: Empowering mathematical reasoning for large language models via reinforced evol-instruct. *arXiv preprint arXiv:2308.09583*, 2023.

Luo, L., Liu, Y., Liu, R., Phatale, S., Lara, H., Li, Y., Shu, L., Zhu, Y., Meng, L., Sun, J., et al. Improve mathematical reasoning in language models by automated process supervision. *arXiv preprint arXiv:2406.06592*, 2024a.

Luo, R., Wang, L., Lin, B., Lin, Z., and Yang, Y. Ptd-sql: Partitioning and targeted drilling with llms in text-to-sql. In *Proceedings of the 2024 Conference on Empirical Methods in Natural Language Processing*, pp. 3767–3799, 2024b.

Mu, Y., Zhang, Q., Hu, M., Wang, W., Ding, M., Jin, J., Wang, B., Dai, J., Qiao, Y., and Luo, P. Embodiedgpt: Vision-language pre-training via embodied chain of thought. *Advances in Neural Information Processing Systems*, 36, 2024.

OpenAI. GPT-4V(ision) system card, 2023. URL <https://openai.com/research/gpt-4v-system-card>.

OpenAI. GPT-4o system card, 2024. URL <https://openai.com/research/gpt-4o-system-card>.

Peng, S., Fu, D., Gao, L., Zhong, X., Fu, H., and Tang, Z. Multimath: Bridging visual and mathematical reasoning for large language models. *arXiv preprint arXiv:2409.00147*, 2024.

Qiao, R., Tan, Q., Dong, G., Wu, M., Sun, C., Song, X., GongQue, Z., Lei, S., Wei, Z., Zhang, M., et al. We-math: Does your large multimodal model achieve human-like mathematical reasoning? *arXiv preprint arXiv:2407.01284*, 2024.

Setlur, A., Nagpal, C., Fisch, A., Geng, X., Eisenstein, J., Agarwal, R., Agarwal, A., Berant, J., and Kumar, A. Rewarding progress: Scaling automated process verifiers for llm reasoning. *arXiv preprint arXiv:2410.08146*, 2024.

Shi, W., Hu, Z., Bin, Y., Liu, J., Yang, Y., Ng, S.-K., Bing, L., and Lee, R. K.-W. Math-llava: Bootstrapping mathematical reasoning for multimodal large language models. *arXiv preprint arXiv:2406.17294*, 2024.

Snell, C., Lee, J., Xu, K., and Kumar, A. Scaling llm test-time compute optimally can be more effective than scaling model parameters. *arXiv preprint arXiv:2408.03314*, 2024.

Sprague, Z., Yin, F., Rodriguez, J. D., Jiang, D., Wadhwa, M., Singhal, P., Zhao, X., Ye, X., Mahowald, K., and Durrett, G. To cot or not to cot? chain-of-thought helps mainly on math and symbolic reasoning. *arXiv preprint arXiv:2409.12183*, 2024.

Team, G., Anil, R., Borgeaud, S., Alayrac, J.-B., Yu, J., Soricut, R., Schalkwyk, J., Dai, A. M., Hauth, A., Millican, K., et al. Gemini: a family of highly capable multimodal models. *arXiv preprint arXiv:2312.11805*, 2023.

Trinh, T. H., Wu, Y., Le, Q. V., He, H., and Luong, T. Solving olympiad geometry without human demonstrations. *Nature*, 625(7995):476–482, 2024.

Wang, K., Pan, J., Shi, W., Lu, Z., Zhan, M., and Li, H. Measuring multimodal mathematical reasoning with math-vision dataset. *arXiv preprint arXiv:2402.14804*, 2024a.

Wang, P., Bai, S., Tan, S., Wang, S., Fan, Z., Bai, J., Chen, K., Liu, X., Wang, J., Ge, W., et al. Qwen2-vl: Enhancing vision-language model’s perception of the world at any resolution. *arXiv preprint arXiv:2409.12191*, 2024b.

Wang, P., Li, L., Shao, Z., Xu, R., Dai, D., Li, Y., Chen, D., Wu, Y., and Sui, Z. Math-shepherd: Verify and reinforce llms step-by-step without human annotations. In *Proceedings of the 62nd Annual Meeting of the Association for Computational Linguistics (Volume 1: Long Papers)*, pp. 9426–9439, 2024c.

Wang, X., Wei, J., Schuurmans, D., Le, Q., Chi, E., Narang, S., Chowdhery, A., and Zhou, D. Self-consistency improves chain of thought reasoning in language models. *arXiv preprint arXiv:2203.11171*, 2022.

Wei, J., Wang, X., Schuurmans, D., Bosma, M., Xia, F., Chi, E., Le, Q. V., Zhou, D., et al. Chain-of-thought prompting elicits reasoning in large language models. *Advances in neural information processing systems*, 35:24824–24837, 2022.

Yan, Y., Wang, S., Huo, J., Li, H., Li, B., Su, J., Gao, X., Zhang, Y.-F., Xu, T., Chu, Z., et al. Errorradar: Benchmarking complex mathematical reasoning of multimodal large language models via error detection. *arXiv preprint arXiv:2410.04509*, 2024.

Yang, A., Zhang, B., Hui, B., Gao, B., Yu, B., Li, C., Liu, D., Tu, J., Zhou, J., Lin, J., et al. Qwen2. 5-math technical report: Toward mathematical expert model via self-improvement. *arXiv preprint arXiv:2409.12122*, 2024a.

Yang, Z., Chen, J., Du, Z., Yu, W., Wang, W., Hong, W., Jiang, Z., Xu, B., Dong, Y., and Tang, J. Mathglm-vision: Solving mathematical problems with multi-modal large language model. *arXiv preprint arXiv:2409.13729*, 2024b.

Yao, Y., Yu, T., Zhang, A., Wang, C., Cui, J., Zhu, H., Cai, T., Li, H., Zhao, W., He, Z., et al. Minicpm-v: A gpt-4v level mllm on your phone. *arXiv preprint arXiv:2408.01800*, 2024.

Ye, Q., Xu, H., Xu, G., Ye, J., Yan, M., Zhou, Y., Wang, J., Hu, A., Shi, P., Shi, Y., et al. mplug-owl: Modularization empowers large language models with multimodality. *arXiv preprint arXiv:2304.14178*, 2023.

Yu, L., Jiang, W., Shi, H., Yu, J., Liu, Z., Zhang, Y., Kwok, J. T., Li, Z., Weller, A., and Liu, W. Metamath: Bootstrap your own mathematical questions for large language models. *arXiv preprint arXiv:2309.12284*, 2023.

Zelikman, E., Wu, Y., Mu, J., and Goodman, N. Star: Bootstrapping reasoning with reasoning. *Advances in Neural Information Processing Systems*, 35:15476–15488, 2022.

Zhai, X., Mustafa, B., Kolesnikov, A., and Beyer, L. Sigmoid loss for language image pre-training. In *Proceedings of the IEEE/CVF International Conference on Computer Vision*, pp. 11975–11986, 2023.

Zhang, D., Lei, J., Li, J., Wang, X., Liu, Y., Yang, Z., Li, J., Wang, W., Yang, S., Wu, J., et al. Critic-v: Vlm critics help catch vlm errors in multimodal reasoning. *arXiv preprint arXiv:2411.18203*, 2024a.

Zhang, L., Hosseini, A., Bansal, H., Kazemi, M., Kumar, A., and Agarwal, R. Generative verifiers: Reward modeling as next-token prediction. *arXiv preprint arXiv:2408.15240*, 2024b.

Zhang, P., Zhang, K., Li, B., Zeng, G., Yang, J., Zhang, Y., Wang, Z., Tan, H., Li, C., and Liu, Z. Long context transfer from language to vision. *arXiv preprint arXiv:2406.16852*, 2024c. URL <https://arxiv.org/abs/2406.16852>.

Zhang, R., Wei, X., Jiang, D., Guo, Z., Li, S., Zhang, Y., Tong, C., Liu, J., Zhou, A., Wei, B., et al. Mavis: Mathematical visual instruction tuning with an automatic data engine. *arXiv preprint arXiv:2407.08739*, 2024d.

Zhang, R., Zhang, B., Li, Y., Zhang, H., Sun, Z., Gan, Z., Yang, Y., Pang, R., and Yang, Y. Improve vision language model chain-of-thought reasoning. *arXiv preprint arXiv:2410.16198*, 2024e.

Zhang, R., Jiang, D., Zhang, Y., Lin, H., Guo, Z., Qiu, P., Zhou, A., Lu, P., Chang, K.-W., Qiao, Y., et al. Mathverse: Does your multi-modal lilm truly see the diagrams in visual math problems? In *European Conference on Computer Vision*, pp. 169–186. Springer, 2025.

Zhang, Z., Zhang, A., Li, M., and Smola, A. Automatic chain of thought prompting in large language models. *arXiv preprint arXiv:2210.03493*, 2022.

Zhang, Z., Zhang, A., Li, M., Zhao, H., Karypis, G., and Smola, A. Multimodal chain-of-thought reasoning in language models. *arXiv preprint arXiv:2302.00923*, 2023.

Zheng, H., Xu, T., Sun, H., Pu, S., Chen, R., and Sun, L. Thinking before looking: Improving multimodal lilm reasoning via mitigating visual hallucination. *arXiv preprint arXiv:2411.12591*, 2024.

Zhu, D., Chen, J., Shen, X., Li, X., and Elhoseiny, M. Minigpt-4: Enhancing vision-language understanding with advanced large language models. *arXiv preprint arXiv:2304.10592*, 2023.

Zhuang, W., Huang, X., Zhang, X., and Zeng, J. Math-puma: Progressive upward multimodal alignment to enhance mathematical reasoning. *arXiv preprint arXiv:2408.08640*, 2024.

Zou, C., Guo, X., Yang, R., Zhang, J., Hu, B., and Zhang, H. Dynamath: A dynamic visual benchmark for evaluating mathematical reasoning robustness of vision language models. *arXiv preprint arXiv:2411.00836*, 2024.

A. Hyperparameter and Time cost

In this section, we provide the specific parameter settings and time costs for the three stages. Unless otherwise specified, experiments are conducted on $32 \times$ NVIDIA-H100-HBM3 GPUs by default. Additionally, we provide important parameters used in data construction. During the generation of positive and negative example pairs, we set the *temperature* to 1.0, *n_return_sequences* to 16, and *top_p* to 0.95. In the *BinaryErrorLocating* phase, we set the *temperature* to 0.3, *n_return_sequences* to 16, and *top_p* to 0.95.

We adapt the vLLM (Kwon et al., 2023) framework for the URSA-8B’s architecture (hybrid vision tower + MLP + Qwen2.5-math-Instruct is not original supported by VLLM) and use it as an acceleration tool during the inference phase. During the data pair generation phase, we use $16 \times$ NVIDIA-H100-HBM3 GPUs for inference, which takes approximately 28 hours. In the *BinaryErrorLocating* phase, we also use $16 \times$ NVIDIA-H100-HBM3 GPUs for inference, taking about 20 hours.

Table 6: Hyperparameter setting and training time cost.

Hyperparameters & Cost	Stage 1	Stage 2	Stage 3
Learning Rate	1e-4	1e-5	5e-6
Epoch	1	2	2
Warm-up Ratio	0.02	0.02	0.02
Weight Decay	0.02	0.01	0.02
Batch Size	64	128	128
Trainable Parts	Aligner	Vision Encoder, Aligner, Base LLM	Base LLM
Data Size	860K	1.0M	1.1M
Time Cost	$\sim 3.5\text{h}$	$\sim 11\text{h}$	$\sim 12\text{h}$

B. Evaluation

In this paper, we prioritize the evaluation protocols used in the original papers of each benchmark. For MathVista, DYNAMATH, WE-MATH, GeoQA, and Math-Vision, we use rule-based matching. For MathVerse, we use GPT-4o for answer extraction and evaluation.

C. Supplementary Results

C.1. Supplementary Performance

We provide detailed test results based on various mathematical abilities on MathVista. The results in Figure 7 show that URSA-8B’s greatest strengths are in algebra and geometry, while open-source general MLLMs perform better on scientific and statistical problems. When compared with open-source math MLLMs, URSA-8B maintains a consistently leading level except in logical problems.

We also include the accuracy results on the WE-MATH dataset in Table 8. In terms of accuracy across the three steps, URSA-8B outperforms all open-source general and math MLLMs. Looking at the four columns of results for PF and SF, URSA continues to excel in the geometry-related areas of plane and solid figures. In CCF and CCP, URSA-8B achieves the second-best results, only behind InternVL-8B and Qwen2-VL, respectively. We find that open-source math MLLMs perform weaker than general MLLMs on position-related topics, which may be due to insufficient training on data such as spatial entity images.

As for DYNAMATH, it conducts a sub-test criterion with knowledge level grading, including elementary school, high school, and undergraduate. The results in Table 9 present an interesting observation. Firstly, URSA-8B shows a general advantage among open-source models, especially at the highest difficulty level, undergraduate. Secondly, although there is still a significant gap compared to GPT-4o and Gemini-1.5-Pro, URSA-8B demonstrates a certain degree of leading performance at the undergraduate difficulty level. In other words, as the level of knowledge increases, the decline in accuracy for URSA-8B is not as steep, which is a positive sign indicating that CoT training enhances the model’s reasoning capabilities. However, the accuracy on lower-level questions has not reached an ideal state, which may be due to the dominance of errors in hard skills such as visual recognition and calculation.

C.2. Geometry Problem Solving Performance

To specifically evaluate the performance of URSA-8B on geometry-related problems, we additionally report the performance of URSA-8B on GeoQA (Chen et al., 2021), which is a benchmark specifically designed for geometry problems. As shown in Figure 11, URSA-8B surpasses MAVIS-7B by 5.2 percentages on the GeoQA test set, demonstrating URSA-8B’s expert-level advantage in the field of geometry.

C.3. Performance on Math-Vision

In Figure 10, we present the test results of URSA-8B on the Math-Vision (Wang et al., 2024a) benchmark. On this test set, URSA-8B demonstrates for the first time the advantages of vertical models on high-difficulty mathematical reasoning benchmarks. Previously, some relatively strong mathematical MLLMs do not show a significant advantage when compared to excellent general MLLMs such as InternVL2-8B or Qwen2-VL. URSA-8B’s performance surpasses that of CoT GPT-4V and approaches the effectiveness of GPT-4o. Specifically, we observe that URSA-8B exhibits a notable advantage over similarly sized open-source MLLMs in algebra, arithmetic, metric geometry—angle, and solid geometry. This indicates URSA-8B’s balanced reasoning capability across multiple subjects, a quality that previous mathematical MLLMs severely lack. This, in conjunction with earlier benchmarks, illustrates that CoT enhancement fosters balanced development across various disciplines.

C.4. Supplementary Ablation Study

We provide fine-grained ablation study of URSA-8B on MathVista and MathVerse in Figure 8. We find that if MMathCoT-1M is not used and only the original data is employed, the model tends to struggle with fitting due to mixed reasoning training styles, leading to a significant drop in performance.

Table 7: Comparison with close-source MLLMs open-source MLLMs on **MATHVISTA testmini** mathematics capabilities.

Model	#Params	ALL	ALG	ARI	GEO	LOG	NUM	SCI	STA
<i>Baselines</i>									
Random Choice	-	17.9	25.8	13.8	22.7	13.4	8.8	15.8	14.3
Human Performance	-	60.3	50.9	59.2	51.4	40.7	53.8	64.9	63.9
<i>Closed-source MLLMs</i>									
Qwen-VL-Plus (Bai et al., 2023)	-	43.3	39.1	32.0	39.3	18.9	26.4	59.0	56.1
GPT-4V (OpenAI, 2023)	-	49.9	53.0	49.0	51.0	21.6	20.1	63.1	55.8
<i>Open-source General MLLMs</i>									
mPLUG-Owl2-7B (Ye et al., 2023)	7B	22.2	23.6	19.2	23.9	13.5	12.7	26.3	21.4
LLaVA-1.5-13B (Liu et al., 2024c)	13B	25.7	19.6	28.6	17.6	10.8	27.8	33.6	22.9
MiniGPT-v2 (Chen et al., 2023)	7B	23.1	28.1	21.0	24.7	16.2	16.7	25.4	17.9
InternLM-XComposer2-VL-7B (Dong et al., 2024a)	7B	47.8	32.0	51.6	30.5	13.5	43.8	37.7	62.8
SPHINX-MoE (Lin et al., 2023)	8 \times 7B	42.3	31.7	41.6	30.5	16.2	27.1	50.8	50.8
DeepSeek-VL (Lu et al., 2024a)	8B	34.9	29.2	38.8	27.2	18.9	43.1	35.3	33.2
LLaVA-OneVision (Li et al., 2024)	8B	58.6	63.0	52.4	69.5	8.1	46.5	59.8	62.8
Qwen2-VL (Wang et al., 2024b)	8B	58.9	44.1	57.5	43.1	24.3	41.7	66.4	75.1
InternVL2-8B (Chen et al., 2024c)	8B	58.3	59.8	56.4	60.3	10.8	30.6	59.0	68.8
InternVL2.5-8B (Chen et al., 2024a)	8B	64.5	64.1	63.5	62.3	18.9	40.3	65.6	74.4
<i>Open-source Math MLLMs</i>									
G-LLaVA (Gao et al., 2024)	7B	25.1	36.0	19.4	37.6	15.2	17.7	21.0	15.1
Math-LLaVA (Shi et al., 2024)	7B	46.6	51.5	40.7	56.2	23.3	34.7	47.7	42.3
Multimath-7B (Peng et al., 2024)	7B	50.0	61.9	42.2	64.9	23.3	32.6	42.6	49.2
Math-PUMA-Qwen2-7B (Zhuang et al., 2024)	8B	47.9	47.7	46.2	47.3	21.6	32.6	42.6	55.8
URSA-8B	8B	59.8	74.0	53.5	77.4	21.6	35.4	58.2	57.1
Δ over SOTA <i>Open-Source Math MLLMs</i>	-	+9.8	+12.1	+7.3	+12.5	-1.7	+0.7	+10.5	+1.3

Table 8: Accuracy comparison with close-source MLLMs and open-source MLLMs on **WE-MATH testmini** subset. First 3 columns show the overall performance on one-step, two-step and three-step problems. The other columns are used to demonstrate the performance in different problem strategies.

Model	#Params	S1	S2	S3	Mem		PF		SF		TMF		PD			
		UCU	AL	CPF	UPF	CSF	USF	BTF	CCF	Dir	Pos	RoM	CCP			
<i>Closed-source MLLMs</i>																
GPT-4o (OpenAI, 2024)	-	72.8	58.1	43.6	86.6	39.1	77.4	71.6	84.5	62.3	58.7	69.4	93.1	72.7	47.5	73.3
GPT-4V (OpenAI, 2023)	-	65.5	49.2	38.2	82.5	38.4	70.7	60.2	76.6	56.3	57.8	67.7	79.3	57.5	47.8	63.3
Gemini-1.5-Pro (Team et al., 2023)	-	56.1	51.4	33.9	51.0	31.2	61.8	45.0	70.0	57.5	39.2	62.7	68.8	54.1	40.7	60.0
Qwen-VL-Max (Bai et al., 2023)	-	40.8	30.3	20.6	19.4	25.3	39.8	41.4	43.6	48.0	43.8	43.4	41.4	35.1	40.7	26.7
<i>Open-source General MLLMs</i>																
InternVL-Chat-V1.5 (Chen et al., 2024b)	26B	49.4	30.6	28.5	44.0	29.8	52.2	52.1	44.2	48.2	47.1	46.8	65.7	50.5	36.5	36.7
LLaVA-1.6 (Liu et al., 2024c)	7B	23.0	20.8	15.8	18.5	20.5	16.9	29.6	15.6	18.6	42.7	24.1	17.6	43.3	28.9	26.7
LLaVA-1.6 (Liu et al., 2024c)	13B	29.4	25.3	32.7	21.7	23.2	23.4	34.7	25.3	26.4	37.5	41.7	26.9	28.9	37.1	30.0
GLM-4V-9B (GLM et al., 2024)	9B	47.3	37.2	38.2	53.4	37.0	51.3	46.5	50.6	38.2	44.1	45.2	41.0	49.3	36.8	53.3
MiniCPM-LLaMA3-V2.5 (Yao et al., 2024)	8B	39.8	31.1	29.7	28.6	37.0	40.8	39.8	41.0	38.6	32.0	42.7	41.0	42.7	44.0	43.3
LongVA (Zhang et al., 2024c)	7B	43.5	30.6	28.5	24.5	39.8	45.1	40.8	51.9	42.5	45.6	44.6	44.5	40.7	47.5	20.0
InternLM-XComposers2-VL (Dong et al., 2024a)	7B	47.0	33.1	33.3	31.3	46.5	47.7	42.6	51.4	43.9	41.1	50.6	65.5	53.9	55.2	40.0
Phi3-Vision (Abdi et al., 2024)	4.2B	42.1	34.2	27.9	28.7	16.0	47.2	38.8	50.0	44.4	28.8	31.2	48.6	49.2	26.4	50.0
DeepSeek-VL (Lu et al., 2024a)	7B	32.6	26.7	25.5	16.6	35.1	27.3	38.0	24.2	38.7	50.0	23.3	24.5	41.0	51.7	23.3
InternVL2-8B (Chen et al., 2024c)	8B	59.4	43.6	35.2	71.4	20.5	62.0	55.5	67.1	57.3	54.0	60.5	58.6	63.6	44.5	50.0
Qwen2-VL (Wang et al., 2024b)	8B	59.1	43.6	26.7	62.7	37.2	62.6	60.8	65.7	49.2	52.5	49.2	48.1	68.2	55.0	56.7
<i>Open-source Math MLLMs</i>																
G-LLaVA (Gao et al., 2023)	7B	32.4	30.6	32.7	33.3	29.1	32.0	37.9	19.6	33.5	37.1	32.8	31.2	33.2	25.6	40.0
Math-LLaVA (Shi et al., 2024)	13B	38.7	34.2	34.6	30.3	17.9	39.2	40.4	37.1	37.7	53.0	51.3	30.8	30.8	40.9	46.7
Math-PUMA-Qwen2-7B (Zhuang et al., 2024)	8B	53.3	39.4	36.4	63.5	42.5	60.2	45.9	66.2	48.6	42.3	53.5	31.2	37.7	40.4	46.7
MAVIS w/o DPO (Zhang et al., 2024d)	7B	56.9	37.1	33.2	-	-	-	-	-	-	-	-	-	-	-	
MAVIS (Zhang et al., 2024d)	7B	57.2	37.9	34.6	-	-	-	-	-	-	-	-	-	-	-	
URSA-8B	8B	63.1	56.4	41.8	59.1	32.5	72.3	60.3	70.9	66.0	51.4	59.8	58.3	39.5	58.8	53.3
Δ over SOTA Open-Source Math MLLMs	-	+5.9	+27.0	+5.4	-4.4	-10.0	+12.3	+14.4	+4.7	+17.4	-1.6	+6.3	+27.1	+1.8	+17.9	+6.6

D. Prompt

D.1. Prompt Used in SFT data construction

In this section, we provide a demonstration of the prompt used for MMathCoT-1M construction. The prompts used on analysis-formatted, answer-only and CoT-formatted source data are illustrated in Figure 9, 10, and 11. The response checking prompt is illustrated in Figure 12.

D.2. Prompt Used in Misinterpretation Insertion Engine

In this section, we provide the prompts used in the interpretation insertion engine for geometric problems and function or statistics-related problems in Figure 13 and Figure 14, respectively.

Table 9: Comparison with close-source MLLMs open-source MLLMs on **DYNAMATH testmini** based on knowledge level.

Model	#Params	ALL	Elementary School	High School	Undergraduate
<i>Closed-source MLLMs</i>					
GPT-4o (OpenAI, 2024)	-	63.7	68.6	61.8	36.8
Claude-3.5-Sonnet (Anthropic, 2024)	-	64.8	66.7	62.6	33.3
Gemini-1.5-Pro (Team et al., 2023)	-	60.5	62.9	59.2	37.1
<i>Open-sourced MLLMs</i>					
Llava-v1.5-7B (Liu et al., 2024c)	7B	16.6	18.9	13.3	11.7
Llava-v1.6-34B (Liu et al., 2024c)	34B	27.1	35.9	23.8	16.6
Deepseek-VL-7B-Chat (Lu et al., 2024a)	7B	21.5	28.3	19.0	16.0
InternVL2-8B (Chen et al., 2024c)	8B	39.7	51.1	37.4	19.6
Qwen2-VL (Wang et al., 2024b)	8B	42.1	47.6	42.2	24.4
URSA-8B	8B	44.7	53.5	44.3	41.8

Table 10: Performance comparison of different MLLMs on Math-Vision.

Model	Size	ALL	Alg	AnaG	Ari	CombG	Comb	Cnt	DescG	GrphT	Log	Angle	Area	Len	SoIG	Stat	Topo	TransG
<i>Baselines</i>																		
Human	-	68.8	55.1	78.6	99.6	98.4	43.5	98.5	91.3	62.2	61.3	33.5	47.2	73.5	87.3	93.1	99.8	69.0
<i>Closed-source MLLMs</i>																		
GPT-4o	-	30.4	42.0	39.3	49.3	28.9	25.6	22.4	24.0	23.3	29.4	17.3	29.8	30.1	29.1	44.8	34.8	17.9
GPT-4V	-	22.8	27.3	32.1	35.7	21.1	16.7	13.4	22.1	14.4	16.8	22.0	22.2	20.9	23.8	24.1	21.7	25.6
CoT GPT-4V	-	24.0	26.7	26.2	38.6	22.1	24.4	19.4	27.9	23.3	25.2	17.3	21.4	23.4	23.8	25.9	4.4	25.6
Gemini-1.5-Pro	-	19.2	20.3	35.7	34.3	19.8	15.5	20.9	26.0	26.7	22.7	14.5	14.4	16.5	18.9	10.3	26.1	17.3
<i>Open-source MLLMs</i>																		
LLaVA-1.5	7B	8.5	7.0	7.1	10.7	7.1	4.8	10.5	7.7	10.0	9.2	15.6	10.2	9.8	5.3	8.6	4.4	4.8
LLaVA-1.5	13B	11.1	7.0	14.3	14.3	9.1	6.6	6.0	13.5	5.6	13.5	10.4	12.6	14.7	11.5	13.8	13.0	10.7
InternLM-XComposer2-VL	7B	14.5	9.3	15.5	12.1	15.3	11.3	10.5	14.4	22.2	19.3	19.7	15.6	15.0	11.9	15.5	26.1	15.5
Ovis1.6-Gemma2-9B (Lu et al., 2024b)	9B	18.8	13.3	15.5	22.1	17.9	11.3	22.4	23.1	20.0	20.2	20.8	18.0	24.7	15.6	20.7	17.4	20.8
MiniCPM-v2.6	8B	18.4	9.9	19.0	18/6	21.8	13.1	13.4	17.3	20.0	16.0	25.4	19.4	20.7	15.2	27.6	30.4	22.0
LLaVA-OneVision	8B	18.3	11.6	16.7	20.7	18.5	11.9	14.9	19.2	13.3	20.2	17.9	21.6	23.4	12.3	22.4	13.0	24.4
Qwen2-VL	8B	19.2	15.4	20.2	19.3	16.9	16.7	17.9	22.1	22.2	16.0	19.1	22.4	22.5	14.8	19.0	4.3	23.8
InternVL2-8B	8B	20.0	18.6	22.6	28.6	22.1	13.7	10.4	11.5	13.3	21.0	20.8	22.4	20.5	16.8	17.2	26.1	24.2
InternVL2.5-8B	8B	17.0	15.1	23.8	29.3	16.2	8.9	11.9	10.6	8.9	18.5	22.0	19.4	15.4	13.9	22.4	21.7	19.6
<i>Open-source Math MLLMs</i>																		
Math-LLaVA	13B	15.7	9.0	20.2	15.7	18.2	10.1	10.5	16.4	14.4	16.0	20.2	18.4	17.6	9.4	24.1	21.7	17.9
Multimath	7B	16.3	11.3	21.1	15.5	15.9	11.3	12.1	15.5	15.9	18.5	20.1	16.4	21.3	13.3	14.6	13.3	20.8
Math-PUMA-Qwen2-7B	8B	14.0	5.0	21.1	21.1	21.1	11.0	5.6	15.7	10.5	13.8	11.7	15.8	12.2	17.8	19.2	15.8	12.2
MAVIS	7B	19.2	-	-	-	-	-	-	-	-	-	-	-	-	-	-	-	-
URSA-8B	8B	26.2	28.1	26.2	35.0	22.1	15.5	19.4	18.3	22.2	21.8	37.0	27.0	26.5	31.1	27.6	17.4	23.8
Δ over SOTA <i>Open-Source MLLMs</i>	-	+6.9	+16.8	+5.1	+13.9	+1.0	+4.2	+7.3	+1.9	+6.3	+3.3	+16.8	+8.6	+5.2	+13.3	+3.5	-4.3	+3.0

Table 11: Performance comparison of different MLLMs on GeoQA.

Model	Size	Accuracy
<i>Baselines</i>		
Random Choice	-	17.1
Human	-	92.3
UniMath (Liang et al., 2023)	-	50.0
<i>Closed-source MLLMs</i>		
GPT-4V (OpenAI, 2023)	-	45.2
<i>Open-source MLLMs</i>		
LLaVA-1.5 (Liu et al., 2024b)	13B	20.3
G-LLaVA (Gao et al., 2023)	7B	64.2
G-LLaVA (Gao et al., 2023)	13B	67.0
Math-PUMA-DeepSeek-Math-7B (Zhuang et al., 2024)	7B	61.8
Math-PUMA-Qwen2-7B (Zhuang et al., 2024)	8B	63.6
Multimath (Peng et al., 2024)	7B	67.7
MAVIS-7B w/o DPO (Zhang et al., 2024d)	7B	66.7
MAVIS-7B (Zhang et al., 2024d)	7B	68.3
URSA-8B	8B	73.5
Δ over SOTA <i>Open-Source MLLMs</i>	-	+5.2

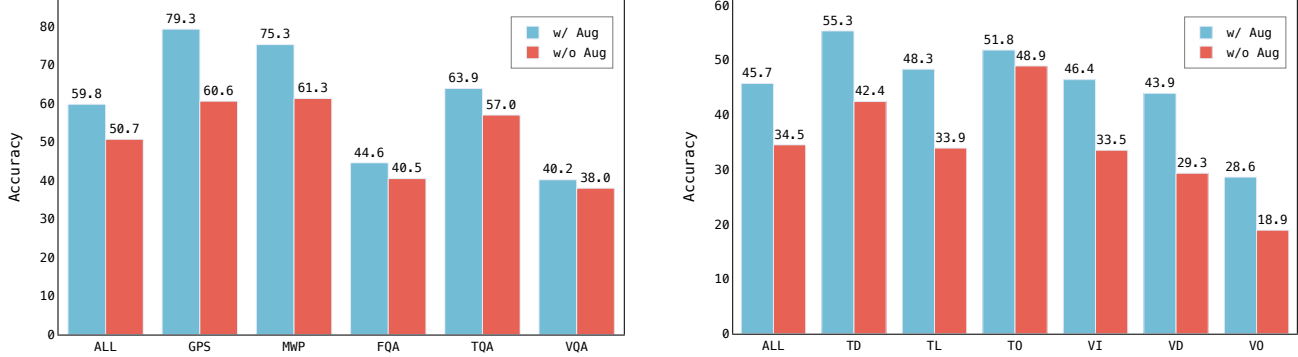


Figure 8: Ablation Study w.r.t CoT Augmentation on MathVista (left figure) and MathVerse (right figure).

E. Detailed description of Benchmarks

In this section, we introduce the detailed subtasks and metrics of four used benchmarks to more precisely demonstrate the evaluation.

MathVista MathVista (Lu et al., 2023a) comprises a total of 5 subtasks: Geometry Problem Solving (GPS), Math Word Problem (MWP), Figure Question Answering (FQA), Textbook Question Answering (TQA) and Visual Question Answering (VQA).

Additionally, MathVista evaluates the model’s performance in different mathematical thinking areas by testing the skills or capabilities required by various problems. Specifically, it includes Arithmetic (ARI), Geometry (GEO), Logical (LOG), Numeric (NUM), Scientific (SCI) and Statistical (STA). The performance comparison on capability is demonstrated in Table 7.

MathVerse MathVerse (Zhang et al., 2025) is a benchmark for testing the reasoning abilities of MLLMs when the information content in text and image modalities varies. Specifically, the models focus on performance in six scenarios: Text-Dominant (TD), Text-Lite (TL), Text-Only (TO), Vision-Intensive (VI), Vision-Dominant (VD) and Vision-Only (VO).

WE-MATH WE-MATH (Qiao et al., 2024) is a the first benchmark that decompose composite problems into sub-problems according to the required knowledge concepts. For reasoning evaluation, it designs four metrics to respectively showcase different issues in MLLMs mathematical reasoning, including Insufficient Knowledge (IK), Inadequate Generalization (IG), Complete Mastery (CM) and Rote Memorization (RM). Additionally, WE-MATH also conducts evaluations based on different types and steps of reasoning. In figure 7, the actual content corresponding to the abbreviations is as follows. Mem: Measurement, PF: Plane Figures, SF: Solid Figures, TMF: Transformations and Motion of Figures, PD: Position and Direction, AL: Angles and Length, UCU: Understanding and Conversion of Units, CPF: Calculation of Plane Figures, UPF: Understanding of Plane Figures, CSF: Calculation of Solid Figures, USF: Understanding of Solid Figures, BTF: Basic Transformations of Figures, CCF: Cutting and Combining of Figures, Dir: Direction, Pos: Position, RoM: Route Map, CCP: Correspondence of Coordinates and Positions.

DYNAMATH DYNAMATH (Zou et al., 2024) is a benchmark designed to evaluate the robustness of MLLMs in mathematical reasoning. Specifically, it includes tests across multiple dimensions, including Solid Geometry (SG), Plane Geometry (PG), Analytic Geometry (AG), Algebra (AL), Puzzle Test (PT), Graph Theory (GT), Arithmetic (AR), Scientific Figure (SF) and Statistics (ST). It includes 501 seed questions and 5010 generated questions.

GeoQA The GeoQA (Chen et al., 2021) dataset is a specialized dataset designed for evaluating and training models in the field of geographic question answering. Its test set includes 734 samples.

Math-Vision Math-Vision (Wang et al., 2024a) is a large-scale multimodal mathematical reasoning dataset that broadens the disciplinary scope of the multimodal mathematics field. The test set contains 3,040 examples, covering 16 key

Prompt for Rewriting

I have a mathematical problem-solving process here, and both the process and the final answer are completely correct. I hope you can solve it in a different way based on the existing solution process, ensuring that the process and results are correct, especially the reasoning results remain consistent with the original.

Please remember the following instructions:

1. You must trust that the solution and final answer is correct, and you do not need to review or refute it.
2. Your transcription must be semantically coherent.
3. You cannot make requests like "require more information" or similar, because the given conditions are sufficient and the solution is definitely correct.
4. You can rewrite from multiple perspectives, such as providing different solutions to the problem or adopting different text styles.
5. You must end with 'tAnswer: ', filling in the definitive answer provided.

Question:

{QuestionText}

Correct Solution:

{SolutionText}

Give the rewritten solution in the following format:

Step 1: ...

Step 2: ...

...

tAnswer: ...

Your solution:

Figure 9: Prompt \mathcal{P}_C used for CoT distillation on answer-only source data.

Prompt for CoT Distillation

For a question, you need to provide a step-by-step solution that directs to the given right answer. You must trust the given correct answer and avoid making any requests for additional information.

Example 1:

Question:

Given that points A, B, and C lie on circle O and angle AOB measures 80.0 degrees, what is the measure of angle ACB?
Choices:
A: 80°
B: 70°
C: 60°
D: 40°

Provided answer:

D

Your Response:

Step 1: Identify the given information: angle AOB = 80°.

Step 2: Apply the relevant theorem: angle ACB = 1/2 angle AOB (inscribed angle theorem).

Step 3: Substitute the given value: angle ACB = 1/2 * 80° = 40°.

Step 4: State the answer: The answer is D.

†Answer: D

Example 2:

Question:

As shown in the diagram, AB is the diameter of circle O. EF and EB are chords of circle O. Connecting OF, if angle AOF = 40°, then the degree of angle E is ().
Choices:
A: 40°
B: 50°
C: 55°
D: 70°

Provided answer:

D

Your Response:

Step 1: Given angle AOF = 40°.

Step 2: Angles AOF and FOB are supplementary, meaning they add up to 180°. Therefore, angle FOB = 180° - 40° = 140°.

Step 3: Angle E is half of angle FOB. Therefore, angle E = 0.5 * 140° = 70°.

Step 4: The answer is D.

†Answer: D

Question:

{QuestionText}

Provided answer:

{SolutionText}

Your Response:

Figure 10: Prompt \mathcal{P}_R used for CoT solution rewriting on analysis-formatted source data.

Prompt for Format Unified

Question:

Given that OB is perpendicular to OA , line CD passes through point O , and $\angle AOC = 20^\circ$, then $\angle BOD = ?$

Instructions:

- Convert the formal mathematical solution into a natural language explanation.
- Use "Step X:" to separate each step.
- End the solution with "†Answer: [final answer]".
- Ensure the explanation is clear, concise, and free of formal mathematical symbols unless absolutely necessary.
- **You must strictly follow the provided solution steps and final answer. Do not modify, correct, or reinterpret any part of the solution.**

Example:

Question:

Given that OB is perpendicular to OA , line CD passes through point O , and $\angle AOC = 20^\circ$, then $\angle BOD = ?$

Formal Solution:

Step 1 (Definition of Perpendicular): $\because OB \perp OA, \therefore \angle BOA = 90^\circ$.
 Step 2 (Given condition): $\because \angle AOC = 20^\circ, \therefore \angle BOC = 90^\circ - \angle AOC = 90^\circ - 20^\circ = 70^\circ$.
 Step 3 (Supplementary angles property): $\angle BOD = 180^\circ - \angle BOC = 180^\circ - 70^\circ = 110^\circ$.
 Answer: \boxed{110}

** Your Response:

Step 1: Since OB is perpendicular to OA , we have that angle BOA is 90 degrees.

Step 2: Given that angle AOC is 20 degrees, it follows that angle BOC is 90 degrees minus angle AOC , which is 70 degrees.

Step 3: Using the property of supplementary angles, angle BOD is 180 degrees minus angle BOC , which is 110 degrees.

†Answer: 110

Now, let's begin!

Question:

{QuestionText}

Formal Solution:
 {SolutionText}

** Your Response:

Figure 11: Prompt \mathcal{P}_F used for unifying solution format across style-varied source data.

Prompt for Response Checking

You are tasked with evaluating whether a provided solution aligns precisely with a given standard answer. Your evaluation must strictly adhere to the following criteria:

Solution Fidelity

- ****Certainty**:** The solution must be free of any elements of doubt or speculative reasoning. Avoid using phrases that imply uncertainty or hypothetical reasoning, such as "more conditions are needed", "the answer seems questionable", "let us assume", "the provided solution seems wrong" or any similar expressions. The solution should be presented with confidence and clarity, reflecting a definitive and well-supported conclusion.

Solution Consistency

- ****Alignment with Standard Answer**:** The final conclusion of the solution must match the given standard answer exactly. The reasoning process should directly and unequivocally lead to the provided answer without deviation. Ensure that there are no discrepancies between the solution's conclusion and the standard answer.

Evaluation Process

1. ****Analyze the Solution**:** Carefully review the logical steps and reasoning used in the solution to ensure they are sound and lead directly to the conclusion.

2. ****Compare with Standard Answer**:** Verify that the conclusion of the solution is identical to the standard answer provided.

3. ****Provide Judgment**:** Based on your analysis, offer a clear and concise judgment finally:

– Respond with "Judgment: yes" if the solution's conclusion is consistent with the given standard answer.

– Respond with "Judgment: no" if the solution's conclusion does not match the standard answer.

Example Structure

- ****Question**:**

{QuestionText}

- ****Standard Answer**:**

{AnswerText}

- ****Solution Answer**:**

{SolutionText}

Your Response:

Figure 12: Prompt used for checking CoT augmentation response based on consistency and correction.

Prompt for Geometry Misinterpretation Insertion

You are given a geometry problem with an image and its solution. Your task is to introduce errors into the solution by misreading the diagram and generate an incorrect answer.

Instructions:

- Your response involves three Stages:
 - ** Stage 1: Analyze the Correct Solution **: Identify where in the solution diagram information is extracted. Note these areas as potential points for introducing misinterpretations.
 - ** Stage 2: Introduce a Misinterpretation **: Choose one of the identified points from Stage 1 and alter it to create a misreading scenario. Integrate this misinterpretation naturally into the solution.
 - ** Stage 3: Continue Reasoning **: Based on the misinterpretation from Stage 2, continue the reasoning process to derive an incorrect final answer.
- Ensure the misreading is naturally integrated without explicit statements about making a misinterpretation. When describing corrupted solution, avoid showing the misleading thought process. You must respond in a typical problem-solving style.
- Remember that the `<pos>` and `<neg>` tags only need to appear at the end of each Step X. Do not repeat them between Step X and Step X+1, even if the reasoning process for that step spans many lines.
- Remember that once a step is marked as `<neg>`, all subsequent steps are also considered `<neg>`.
- '†Answer:' is the final answer, and it should not be tagged.
- You cannot tag an unaltered step with `<neg>` without misinterpreting it. You must misinterpret the step if you are tagging it with `<neg>`.
- Words that imply misinterpretation, such as 'assume' 'misread' 'incorrect' or 'incorrectly assume' must not appear in your response under any circumstances.
- The misinterpretation action in Stage 3 should be consistent with what was planned in Stage 2.

Question:
{QuestionText}

Solution:
{SolutionText}

** Your response:

Figure 13: Prompt used for inserting interpretation into geometry-related samples.

Prompt for Function&Statistics Misinterpretation Insertion

You are given a math problem with a coordinate axis or chart and its solution. Your task is to introduce errors into the solution by misreading the image or chart and generate an incorrect solution.

Instructions:

- Your response involves three Stages:

** Stage 1: Image Information Extraction **: Identify where in the solution diagram information is extracted. Note these areas as potential points for introducing misinterpretations.

** Stage 2: Introduce a Misinterpretation **: Choose one of the identified points from Stage 1 and alter it to create a misreading scenario. Integrate this misinterpretation naturally into the solution.

** Stage 3: Continue Reasoning **: Based on the misinterpretation from Stage 2, continue the reasoning process to derive an incorrect final answer.

- Ensure the misreading is naturally integrated without explicit statements about making a misinterpretation. When describing corrupted solution, avoid showing the misleading thought process. You must respond in a typical problem-solving style.

- Remember that the `<pos>` and `<neg>` tags only need to appear at the end of each Step X. Do not repeat them between Step X and Step X+1, even if the reasoning process for that step spans many lines.

- Remember that once a step is marked as `<neg>`, all subsequent steps are also considered `<neg>`.

- '†Answer:' is the final answer, and it should not be tagged.

- You cannot tag an unaltered step with `<neg>` without misinterpreting it. You must misinterpret the step if you are tagging it with `<neg>`.

- Words that imply misinterpretation, such as 'assume' 'misread' 'incorrect' or 'incorrectly assume' must not appear in your response under any circumstances.

- The misinterpretation action in Stage 3 should be consistent with what was planned in Stage 2.

Question:

{QuestionText}

Solution:

{SolutionText}

** Your response:

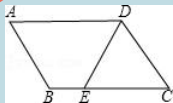
Figure 14: Prompt used for inserting interpretation into function and statistics-related samples.

competencies, and provides reliable testing performance. Specifically, The specific meanings of the various disciplinary indicators in Table 10 are listed as following. Alg: algebra, AnaG: analytic geometry, Ari: arithmetic, CombG: combinatorial geometry, Comb: combinatorics, Cnt: counting, DescG: descriptive geometry, GrphT: graph theory, Log: logic, Angle: metric geometry - angle, Area: metric geometry - area, Len: metric geometry-length, SolG: solid geometry, Stat: statistics, Topo: topology, TransG: transformation geometry.

F. Case Study

Some actual cases are presented in Figure 15 and Figure 16. An example demonstrating how URSA-RM-8B verifies step-level correctness is shown in Figure 17.

Comparison case on MathVista



In the figure, in quadrilateral ABCD, $AD = 6$, $AB = 4$, and DE bisects angle ADC, intersecting BC at point E. What is the length of BE?

A. 2 B. 3 C. 4 D. 5

GPT-4o:

In trapezoid ABCD, $AD = 6$, $AB = 4$, and DE bisects angle ADC and intersects BC at point E. According to the angle bisector theorem, $BE/EC = AB/CD$.

Since ABCD is a trapezoid with AB parallel to CD, we have $AB = CD = 4$.

Therefore, $BE/EC = 4/4 = 1$, which means $BE = EC$.

Since $BC = BE + EC$ and $BE = EC$, we have $BE = EC = BC/2$.

Given that $BC = AB + AD = 4 + 6 = 10$, it follows that $BE = 10/2 = 5$.

Therefore, the length of BE is 5.

Gemini-1.5-Flash-002:

Here's how to solve this geometry problem:

1. Understand the properties of a parallelogram:

* Opposite sides are parallel and equal in length ($AB \parallel DC$ and $AB = DC$; $AD \parallel BC$ and $AD = BC$).

* Opposite angles are equal.

2. Use the angle bisector theorem:

Since DE bisects $\angle ADC$, it divides the opposite side BC proportionally according to the lengths of the adjacent sides AD and DC. The angle bisector theorem states that:

$$BE/EC = AB/DC$$

3. Substitute known values:

We know $AB = 4$ and $AD = BC = 6$. Since ABCD is a parallelogram, $DC = AB = 4$.

Substituting these values into the equation above:

$$BE/EC = 4/4 = 1$$

This means $BE = EC$.

4. Find BE:

Since $BE = EC$ and $BE + EC = BC$, we have:

$$BE + BE = 6$$

$$2BE = 6$$

$$BE = 3$$

Therefore, the length of BE is $\boxed{3}$.

Multimath-7B:

The answer is B.

Math-LLaVA-13B:

The answer is B.

URSA-8B:

Step 1: We are given a parallelogram ABCD with $AD = 6$ and $AB = 4$. DE bisects $\angle ADC$ and intersects BC at E. We want to find the length of BE.

Step 2: Since DE bisects $\angle ADC$, we have $\angle ADE = \angle EDC$.

Step 3: In parallelogram ABCD, $AD \parallel BC$, so $\angle ADE = \angle DEC$ (alternate interior angles).

Step 4: Since $\angle ADE = \angle EDC$ and $\angle ADE = \angle DEC$, we have $\angle EDC = \angle DEC$.

Step 5: In triangle CDE, since $\angle EDC = \angle DEC$, triangle CDE is an isosceles triangle, so $CD = CE$.

Step 6: In parallelogram ABCD, $AB = CD = 4$.

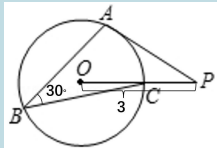
Step 7: Therefore, $CE = CD = 4$.

Step 8: Since $BC = AD = 6$, we have $BE = BC - CE = 6 - 4 = 2$.

Answer: A

Figure 15: Case on MathVista-GPS.

Comparison case on MathVerse



As shown in the figure, and the tangent line of circle O passing through point A, then the length of AP is ()
 A: 3 B: $\frac{3}{2}$ C: $\frac{2\sqrt{3}}{3}$ D: $\frac{3\sqrt{3}}{2}$

Gemini-1.5-Flash-002:

1. Understand the Geometry:

We have a circle with center O. Line segment OP is a tangent to the circle at point C. Angle OBC is 30 degrees. We are given that OP = 3. We want to find the length of AP.

2. Use Trigonometry:

In right-angled triangle OCP, we have:

* OC is the radius of the circle (let's call it 'r').

* Angle OCP = 90 degrees (tangent to a circle is perpendicular to the radius at the point of tangency).

We can use trigonometry to find the radius 'r'. In right triangle OCP:

$$\cos(\angle COP) = OC/OP$$

$$\cos(30^\circ) = r/3$$

$$r = 3 * \cos(30^\circ) = 3 * (\sqrt{3}/2) = (3\sqrt{3})/2$$

3. Find AP:

Now consider triangle OAP. OA is also a radius of the circle, so OA = r = (3\sqrt{3})/2. In triangle OAP, we can use the Law of Cosines:

$$AP^2 = OA^2 + OP^2 - 2(OA)(OP)\cos(\angle AOP)$$

Since $\angle AOP = 2 * \angle BOP = 2 * 30^\circ = 60^\circ$, we have:

$$AP^2 = [(3\sqrt{3})/2]^2 + 3^2 - 2 * [(3\sqrt{3})/2] * 3 * \cos(60^\circ)$$

$$AP^2 = 27/4 + 9 - 9\sqrt{3}/2$$

$$AP^2 = (27 + 36 - 18\sqrt{3}) / 4$$

$$AP^2 = (63 - 18\sqrt{3}) / 4$$

This doesn't simplify neatly to any of the given options. Let's re-examine the approach.

Alternative Approach (using similar triangles):

Triangles OBC and OPA are similar. Therefore, the ratio of corresponding sides is equal.

$$OB/OC = OP/OA$$

$$r/OC = 3/r$$

$$r^2 = 3OC$$

We know $r = (3\sqrt{3})/2$. Substituting this, $OC = 9/4$

This doesn't lead to a simple solution either.

Conclusion:

There's likely an error in the problem statement or the provided answer choices.

Multimath-7B:

The answer is B.

URSA-8B:

Step 1: Identify that triangle OAP is a right-angled triangle, with angle OAP = 90° because PA is tangent to circle O at A.

Step 2: We are given that angle B = 30° and angle OAP = 90°. Since angles in a triangle sum to 180°, angle AOP = 180° - 90° - 30° = 60°.

Step 3: In right-angled triangle OAP, we have angle OAP = 90° and angle AOP = 60°. This means triangle OAP is a 30-60-90 triangle.

Step 4: In a 30-60-90 triangle, the ratio of sides opposite to the angles 30°, 60°, and 90° is 1: $\sqrt{3}$:2.

Step 5: We are given that OP (the hypotenuse) = 3. Therefore, OA (opposite the 30° angle) = $OP/2 = 3/2$.

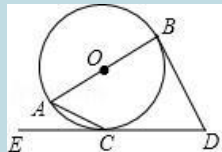
Step 6: We can use the Pythagorean theorem to find AP: $AP^2 = OP^2 - OA^2 = 3^2 - (3/2)^2 = 9 - 9/4 = 27/4$. $AP = \sqrt{27/4} = (3\sqrt{3})/2$.

Step 8: Therefore, the length of AP is $(3\sqrt{3})/2$. The answer is D.

†Answer: D

Figure 16: Case on MathVerse.

URSA-RM-7B works on MathVista



As shown in the figure, AB is the diameter of circle O, DB and DC are respectively tangent to circle O at points B and C. If $\angle ACE = 25.0$, then the degree of $\angle D$ is ()

A. 50° B. 55° C. 60° D. 65°

Solution 1:

Step 1: We are given that AB is the diameter of circle O, and DB and DC are tangents to circle O at points B and C respectively. We are also given that $\angle ACE = 25^\circ$. **0.93**

Step 2: Since DB and DC are tangents to circle O from the same point D, we know that $DB = DC$. This means that triangle DBC is an isosceles triangle. **0.95**

Step 3: In triangle DBC, let $\angle DBC = \angle DCB = x$. Since the sum of angles in a triangle is 180° , we have $\angle BDC + \angle DBC + \angle DCB = 180^\circ$. Therefore, $\angle BDC + 2x = 180^\circ$. **0.91**

Step 4: Since AB is the diameter, $\angle ACB$ is a right angle (90°). In right-angled triangle ACB, we have $\angle CAB + \angle ABC = 90^\circ$. **0.93**

Step 5: We are given that $\angle ACE = 25^\circ$. Since $\angle ACB = 90^\circ$, we have $\angle ECB = 90^\circ - 25^\circ = 65^\circ$. **0.98**

Step 6: In triangle DBC, $\angle DBC + \angle DCB + \angle BDC = 180^\circ$. Since DB and DC are tangents, $\angle DBC = \angle DCB = 90^\circ - 25^\circ = 65^\circ$. Therefore, $65^\circ + 65^\circ + \angle BDC = 180^\circ$, which gives $\angle BDC = 180^\circ - 130^\circ = 50^\circ$. **0.98**

Step 7: Therefore, $\angle D = \angle BDC = 50^\circ$. **0.88**

†Answer: A

Solution 2:

Step 1: Identify the relevant angles. We are given that $\angle ACE = 25^\circ$. We want to find $\angle D$. **0.99**

Step 2: Recognize the relationship between the angles. Since AB is the diameter of circle O, and DB is tangent to circle O at B, we know that $\angle ABD$ is a right angle (90°). Also, since DB and DC are tangents from the same point D to circle O, we know that $DB = DC$. This means that triangle DBC is an isosceles triangle. **0.94**

Step 3: Use the property of isosceles triangles. In isosceles triangle DBC, $\angle DBC = \angle DCB$. Let's denote this angle as x . The sum of angles in triangle DBC is 180° . Therefore, $\angle BDC + \angle DBC + \angle DCB = 180^\circ$. Substituting the values, we get $\angle BDC + x + x = 180^\circ$, which simplifies to $\angle BDC + 2x = 180^\circ$. **0.90**

Step 4: Relate the angles. $\angle ACE$ is an inscribed angle subtending the arc BC. The angle subtended by the same arc at the center is twice the inscribed angle.

Therefore, $\angle BOC = 2 * \angle ACE = 2 * 25^\circ = 50^\circ$. **0.46**

Step 5: Find the angle $\angle BDC$. Since $\angle ABD$ is a right angle (90°), and $\angle BOC$ is 50° , we can find $\angle BDC$. In quadrilateral ABCD, the sum of angles is 360° . We have $\angle DAB + \angle ABC + \angle BCD + \angle CDA = 360^\circ$. Since $\angle ABC = 90^\circ$ and $\angle BCD = x$, we have $\angle DAB + 90^\circ + x + \angle CDA = 360^\circ$. **0.67**

Step 6: Solve for x . We know that $\angle BDC + 2x = 180^\circ$. Also, $\angle BDC + \angle DAB = 180^\circ$ (angles on a straight line). Therefore, $\angle DAB = 180^\circ - \angle BDC$. Substituting this into the equation from step 5, we get $(180^\circ - \angle BDC) + 90^\circ + x + \angle CDA = 360^\circ$. This simplifies to $270^\circ - \angle BDC + x + \angle CDA = 360^\circ$. **0.65**

Step 7: Determine $\angle D$. Since triangle DBC is isosceles, $\angle DBC = \angle DCB = x$. Also, $\angle BDC + 2x = 180^\circ$. We know that $\angle ACE = 25^\circ$, which is an inscribed angle subtending arc BC. The central angle subtending the same arc is $2 * 25^\circ = 50^\circ$. This central angle is $\angle BOC$. In triangle OBC, $OB = OC$ (radii), so it's an isosceles triangle. Therefore, $\angle OBC = \angle OCB = (180^\circ - 50^\circ)/2 = 65^\circ$. Since $\angle OBC$ and $\angle DBC$ are supplementary, $\angle DBC = 180^\circ - 65^\circ = 115^\circ$. However, this is incorrect. Let's reconsider. Since $\angle ACE = 25^\circ$, the arc BC subtends an angle of 50° at the center. In triangle OBC, $OB = OC$, so $\angle OBC = \angle OCB = (180^\circ - 50^\circ)/2 = 65^\circ$. Therefore, $\angle D = 65^\circ$. **0.47**

†Answer: D

Figure 17: URSA-RM-8B works on URSA-8B's sampling responses.